https://doi.org/10.5194/bg-2020-401
Preprint. Discussion started: 28 December 2020

Biogeosciences Discussions

Versatile soil gas concentration and isotope monitoring: optimization and integration of novel soil gas probes with online trace gas detection

Juliana Gil-Loaiza[1], Joseph R. Roscioli[2], Joanne H. Shorter[2], Till H. M. Volkmann[3,4], Wei-Ren Ng[3], Jordan E. Krechmer[2], Laura K. Meredith[1,3,*]

[1] School of Natural Resources and the Environment, University of Arizona, Tucson, AZ, 85721, USA
[2]Aerodyne Research Inc., Billerica, MA, 01821, USA
[3]Biosphere 2, University of Arizona, Oracle, AZ, 85623, USA
[4]Applied Intelligence, Accenture, Kronberg im Taunus, Hesse, 61476, Germany.

Correspondence to: Laura K. Meredith laurameredith@email.arizona.edu

Abstract. Gas concentrations and isotopic signatures can unveil microbial metabolisms and their responses to environmental changes in soil. Currently, few methods measure soil trace gases such as the products of nitrogen and carbon cycling, or volatile organic compounds (VOCs), that could constrain microbial biochemical processes like nitrification, methanogenesis, respiration, and microbial communication. Versatile trace gas sampling systems that integrate soil probes with sensitive trace gas analyzers could fill this gap with measurements resolving spatial (centimeter scale) and temporal (minutes) variations in concentrations and isotopic signatures of in situ soil gases. We developed a system that integrates new 15 cm long sintered PTFE diffusive soil gas probes with various infrared spectrometers and a VOC mass spectrometer. The system is based on porous and hydrophobic soil probes that non-disruptively collect and transport gas from multiple probes to one or more central gas analyzers. Here, we demonstrate the feasibility and versatility of an automated multi-probe system for soil gas measurements of isotopic ratios of nitrous oxide ($\delta^{18}O$, $\delta^{15}N$, and the ^{15}N site-preference of N_2O), methane, carbon dioxide ($\delta^{13}C$), and VOCs. First, we used an inert silica matrix to challenge probe measurements under controlled gas conditions. By changing and controlling system flow parameters, including probe flow rate, we optimized recovery of representative soil gas samples while reducing sampling artifacts on subsurface concentrations. Second, we forced environmental manipulations in soil-filled columns to demonstrate real time detection of subsurface gas dynamics in response to irrigation and soil redox conditions. In addition, we developed a new laser spectrometer to recover isotope ratios for $^{14}N^{14}N^{16}O$ ("δ446"), $^{14}N^{15}N^{16}O$ ("δ456"), $^{15}N^{14}N^{16}O$ ("δ546"), and $^{14}N^{14}N^{18}O$ ("δ448") with high precision and low concentration dependence. We captured temporal subsurface gas pulses in CO_2, N_2O, and VOCs. This demonstrated the potential for diffusive-based probes to couple to trace gas sensors for soil health and fertility studies, and to inform high-throughput meta-omics, leading to the development of a suite of powerful new tools for soil analysis.

https://doi.org/10.5194/bg-2020-401
Preprint. Discussion started: 28 December 2020


Biogeosciences Discussions

1 Introduction

The impact of soil gas fluxes on atmospheric composition is typically measured at the soil surface, yet new belowground approaches may provide a more mechanistic perspective of trace gas cycling. Soil is a source and sink of important trace gases including nitrous oxide (N_2O), carbon dioxide (CO_2), methane (CH_4), and volatile organic compounds (VOCs). Soil fluxes are driven by abiotic and biotic processes including microbial metabolism, and soil environmental conditions (Conrad, 2005; Jiao et al., 2018; Karbin et al., 2015), both of which vary in space (i.e. soil aggregate (Schimel, 2018) to field (Wang et al., 2014) and time (e.g. rain-driven N_2O emission pulses). For example, carbon and nitrogen cycling processes that produce CO_2 (respiration), CH_4 (methanogenesis), N_2O (denitrification), and volatile organic compounds (VOCs) are affected by variables including temperature, oxygen level, soil moisture, and nutrient availability that can change on a fine spatial scale in a short period of time (Jiao et al., 2018). Soil moisture and oxygen modulate denitrification processes in soil, and hence emissions of N_2O (Groffman et al., 2009) and VOCs (e.g. butane, benzene, and methanol (Abis et al., 2020; Raza et al., 2017)). Soil conditions also affect CH_4 production and consumption from microbial communities at micron to centimeter scales (Schimel, 2018). These spatial and temporal variations in belowground processes strongly influence subsurface gas dynamics, yet constraining how this belowground variability affects soil fluxes has been limited by an inability to make real time and in situ measurements. As a result, the contribution of processes and influence of drivers to net surface fluxes remains buried.

In addition to contributing to atmospheric composition via above-ground fluxes, soil gases serve as messengers of belowground biogeochemical processes and microbial activity. Soil microbial metabolism produces specific trace gases via biochemical pathways that impart characteristic isotopic signatures to trace gas moieties. Measurements of stable isotopomers (abundance and position) of soil trace gases can therefore be a valuable tool to identify and quantify gas processes (Yoshida and Toyoda, 2000). For example, the CH_4 production pathway (acetoclastic, hydrogenotrophic, or methylotrophic methanogenesis) can be identified by the ratio of rare $^{13}CH_4$ to the abundant $^{12}CH_4$ (McCalley et al., 2014; Penger et al., 2012)). Similarly, the ratio of ^{15}N to ^{14}N, and the position of the ^{15}N relative to the O in N_2O depends upon its production pathway, such as hydroxylamine decomposition, chemodenitrification, nitrifier denitrification, or denitrifier denitrification (Sutka et al., 2006; Yoshida and Toyoda, 2000). Measurements of all three isotopic properties of N_2O (^{15}N abundance, ^{15}N site preference, and ^{18}O abundance) can identify the type of biochemical process generating the N_2O, and the microbe type (bacterial, archaeal, or fungal) (Toyoda et al., 2017). VOCs are signals for diverse microbial and chemical interactions in soils. They are metabolites and signaling molecules involved in microbial and plant-microbe interactions such as quorum sensing, and they can reflect soil health, stress responses, and microbial identity (Insam and Seewald, 2010; Schulz-Bohm et al., 2018). Advances in tracking soil microbial activity using trace gas messengers will elevate the understanding of the role of microbial communities and their metabolism in soil health, greenhouse gas cycling, and biological interactions in soil.

Over the years, soil gas sampling approaches have evolved to recover gas samples with less disruption to the soil environment. Early soil gas sampling methods inserted rigid perforated tubes or wells into the soil to withdraw soil gas by

https://doi.org/10.5194/bg-2020-401
Preprint. Discussion started: 28 December 2020

suction using a syringe (Holter, 1990), pump (Maier et al., 2012), or other manual sampling method (Panikov et al., 2007). This methodology to extract gas from the soil pores was time consuming and created artifacts by driving advective flow, disturbing the probe surroundings, transporting gas beyond the probe area compromising the real gas concentration (Maier et al., 2012), and in some cases, withdrawing insufficient sample volume for analysis. To overcome the drawbacks of advective gas sampling, diffusive probes sample soil gases by non-advective gas exchange driven by molecular diffusion across a diffusive membrane. Porous membranes allow the partitioning of the gas from soil and liquid phases (Volkmann et al., 2016a, 2016b). One drawback of diffusive sampling probes has been the relatively large volume needed to generate sufficient sample for gas analyzers and the correspondingly long time required for the internal sampling volume to reach equilibration with soil gas. For example, probes larger than 1 m have been used in water (Rothfuss et al., 2013) and soil (Jacinthe and Dick, 1996), and small silicone probes have required extended sampling times (>7-48 hours) to equilibrate (Kammann et al., 2001) (Petersen, 2014). Polypropylene (Accurel, V8/2HF, Membrana GmbH, Germany) materials improved equilibrium time at an equivalent probe length (Flechard et al., 2007; Gut et al., 1998; Rothfuss et al., 2013). Long probes disturb soil, especially upon installation, spurring the interest in discovering new materials that enhance diffusion at a smaller probe size while still resolving gas concentrations and isotopic signatures. For example high density materials like expanded polytetrafluoroethylene (PTFE), and polyethylene promote better equilibration time than silicone (DeSutter et al., 2006) increasing temporal resolution from hours to minutes in different matrices, e.g. water isotopes in soil (Volkmann and Weiler, 2014) and tree xylem (Volkmann et al., 2016a), and CO_2 in soil (DeSutter et al., 2006). These materials recovered representative gas concentrations and isotopic signatures, but have been limited by cracking, water infiltration (Volkmann et al., 2016a, 2016b), and soil disruption during sampling (Hirsch et al., 2004). Nonetheless, diffusive sampling approach is a promising means for non-destructively recovering soil gas for analysis. The search is ongoing for materials that equilibrate efficiently by diffusion with minimal probe length.

Probes face multiple demands in the soil system during field deployment. For long-time monitoring in the field, subsurface probes must be robust to extreme weather, plant and microbial activity, and other site disruptions that could affect the integrity of the porous membrane. The probe material must tolerate environmental changes and interactions with biotic and abiotic factors. Microbial interactions with probe materials can reduce probe integrity (Rothfuss and Conrad, 1994), modify gas concentrations, or reduce gas exchange by biofouling (Krämer and Conrad, 1993). Small soil particles can clog probe pores and limit gas diffusion and probes can also break or crack in freeze-thaw cycles (Burton and Beauchamp, 1994; Gut et al., 1998) or during installation (Volkmann et al., 2016a, 2016b). Probe membranes must resist water break-through, which has caused water interference problems in nylon (Burton and Beauchamp, 1994) and polypropylene (Gut et al., 1998) probes. The limitations of some probe materials have been evaluated under controlled conditions (DeSutter et al., 2006; Munksgaard et al., 2011; Rothfuss et al., 2013). To address these challenges, new non-reactive and hydrophobic porous probe material is needed to meet the demands of long-term soil sampling.

An advantage of diffusive soil gas probes is that they can be integrated with online soil gas sampling instrumentation to quantify soil gas concentrations and isotopic signatures (Gangi et al., 2015; Gut et al., 1998; Rothfuss et al., 2013; Volkmann

https://doi.org/10.5194/bg-2020-401
Preprint. Discussion started: 28 December 2020


Biogeosciences Discussions

et al., 2016b, 2018). So far, a fraction of available trace gas analyzers have been integrated with online (e.g. H_2O, CO_2, CH_4) diffusive soil gas sampling systems, leaving the majority of gas cycling and microbial messengers untapped. Tunable Infrared Laser Direct Absorption Spectrometers (TILDAS) measure important small molecules such as N_2O, CH_2, NO, CO_2, and CO. VOCs, valuable markers of different and highly specific biogeochemical processes, can be monitored with Proton Transfer Reaction Time Of Flight Mass Spectrometers (PTR-TOF-MS). There is a need to test sampling systems under controlled conditions with promising new probe materials to integrate with the diverse suite of available high precision gas analyzers. The methods should be optimized for different gases, recognizing differences in molecular diffusivity (exchange across probe) and surface interactions (partitioning to tubing). Online, multiplexed systems have been deployed in the field to measure multiple spatial points (Jochheim et al., 2018; Volkmann and Weiler, 2014). Expanding the gases that can be sampled by diffusive soil gas sampling probes in the field will increase understanding of biogeochemical processes through measurements at a refined temporal and spatial resolution.

In this study, we describe a real time soil trace gas sampling system that integrates diffusive soil probes with TILDAS and PTR-TOF-MS Vocus analyzers to capture fast, spatially resolved production and isotopic signatures of key soil trace gases and their responses to environmental changes. To achieve this, we developed diffusive, hydrophobic soil probes from sintered PTFE (sPTFE) and used custom controlled soil columns to evaluate their ability to retrieve gas samples via continuous sampling. We measured trace gas messengers of microbial nitrogen and carbon cycling (N_2O, CH_4, CO, CO_2,,VOCs), including the site-specific stable isotopologues of N_2O and CH_4. The sPTFE probe material has uniform pore distribution, improving gas diffusion, and is chemically and biologically inert and terminally resistant, properties that make this material a good candidate for long term soil gas probes. We evaluated the integration of the probe and the analyzers using columns with (i) a silica matrix with controlled gas concentrations, and (ii) a soil matrix with manipulated environmental conditions, mimicking precipitation and changing redox conditions of the soil. In addition, we optimized the TILDAS sample cell volume, sample transfer schemes and flow rates, and the instrument's concentration dependence. Here, we show that improving soil gas sampling methods and coupling to online high-resolution instrumentation can lead to a robust and flexible system that measures a wide array of soil trace gases and will give a snapshot of microbial activity and biogeochemical cycles in soils.

https://doi.org/10.5194/bg-2020-401
Preprint. Discussion started: 28 December 2020

2. Materials and Methods

2.1 Probes and prove evaluation system

2.1.1 Sintered PTFE (sPTFE) probes

We built gas permeable soil probes from microporous tubes of sPTFE (Fig. 1a). sPTFE is hydrophobic, allowing gas diffusion across the tube while preventing liquid water breakthrough. The material is structurally stable and non-reactive making it suitable for long-term use in soils. We selected a total of four probes with different pore sizes and tube dimensions including the outer diameter, inner diameter, and wall thickness (Table 1) to evaluate their equilibration properties and soil impacts. Probes were machined (White Industries, Inc., Petaluma, CA) from solid sPTFE blocks (Berghof GmbH, Eningen, Germany). In some cases probes were made from two pieces (Table 1) assembled as a single probe using perfluoroalkoxy (PFA) unions (Swagelok, Solon, OH). We constructed probe prototype assemblies to connect probes to inlet and outlet transport lines of 1/8" fluorinated ethylene propylene (FEP, Versilion™, Saint-Gobain, Malvern, PA) using stainless steel reducing unions (Swagelok, Solon, OH). In some cases, PTFE tape was used to account for mismatch between fittings and probe outer diameters. After assembly, each probe was submerged under water while flowing ultra-zero air gas through the probe test for leaks in the fitting assembly. This was to ensure that probe sample concentrations were the result only of gas diffusion across the porous wall of the probe.

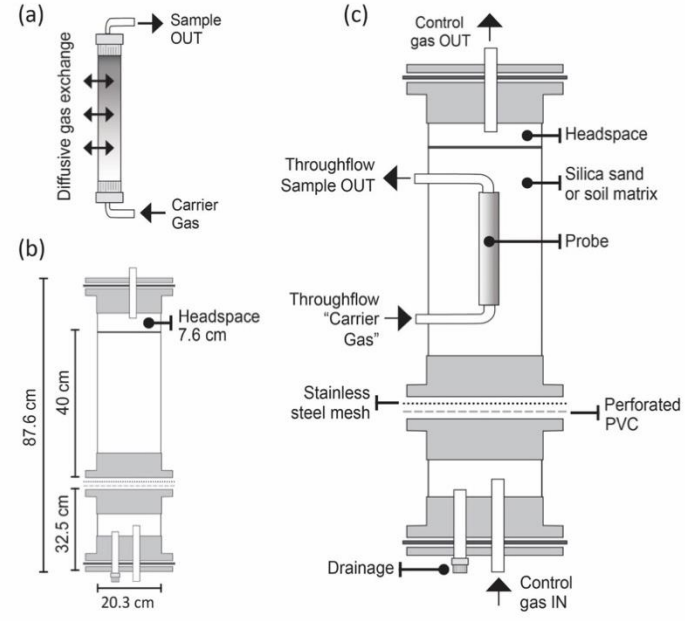

Figure 1. Lab-based custom soil column assembly built to evaluate probe performance against controlled gas concentrations in a silica sand and soil matrix. (a) microporous probe of sPTFE, (b) dimensions of the two column sections, and (c) column components to enable controlled probe evaluation.

https://doi.org/10.5194/bg-2020-401
Preprint. Discussion started: 28 December 2020

Table 1. List of sPTFE probe pore size and dimensions including outer diameter (OD), inner diameter (ID), and wall thickness (W)

Probe ID (pore size in µm)	Dimensions (mm) (OD x ID x W)	Length (mm)
P5 (5)	12.7 x 6.3 x 1.6	147.5
P8 (8)	12.7 x 6.3 x 1.6	147.5
P10 (10)	12.7 x 6.3 x 1.6	147.5
P25* (25)	9.5 x 4.7 x 2.4	147.5

* Two sPTFE pieces joined with a PFA fitting

2.1.2 Soil Columns

We built experimental columns to (1) evaluate probe performance under controlled gas supply and in a non-reactive matrix (silica sand), and (2) measure in situ gas dynamics in response to environmental manipulations (e.g. wetting, redox state) in a complex matrix (soil). Our custom soil columns allowed a gas of controlled composition (control gas) to be advectively forced through the matrix from below (Fig. 1). We placed silica sand in the columns and continuously flushed them with known gas concentrations and isotope ratios to evaluate probe performance (System 1 tests at University of Arizona; UA, and System 2 tests at Aerodyne Research Inc., ARI, Section 2.3.1). We also used the columns to drive controlled environmental manipulations including controlled wetting and forced shifts from anaerobic to aerobic conditions to measure in situ gas dynamics in complex soil (System 2 tests at ARI, Section 2.3.2).

Each column consisted of two sections (Fig. 1b): a lower section (32.5 cm) supporting drainage and buffered delivery of control gas, and an upper section (40 cm) containing the matrix (silica or soil), with a headspace layer for uniform column outflow (7.6 cm). Together, the two column sections were 20.3 cm inner diameter, 87.6 cm length (including base and cover), 28 L volume and constructed from schedule 80 PVC. The central location of the probe in the upper section allowed sufficient distance from column walls (10 cm) and the soil/gas interface (15.2 cm) to avoid edge effects (Fig. 1c). The upper and lower column sections were separated by a layer of perforated PVC (staggered 1/8 in. holes and 40% open area) and a type 304 stainless steel wire cloth mesh (325 x 325 mesh (44 µm), 0.051 mm opening size) to allow passage of control gas and drainage of water, while retaining matrix integrity in the upper section. During controlled irrigation experiments, excess water in the matrix dripped into the lower section and out a drain on the base (sealed during sampling). Column sections were joined using schedule-80 PVC flanges, bolts, and rubber gasket seals allowing columns to be modular and easy to disassemble, transport,

https://doi.org/10.5194/bg-2020-401
Preprint. Discussion started: 28 December 2020

and refill. Additionally, PTFE and polyetheretherketone (PEEK) bulkhead fittings (IDEX Health & Science LLC., Oak Harbor, WA, USA) and washers provided air-and water tight connections for the sampling and control gas tubing. The gas permeable soil probes were installed in the center of the column, and can be flanked by soil sensors (e.g. moisture, temperature) (Fig. 1c).

Silica sand (Granusil 4095; high purity industrial quartz; Covia Corporation, Emmett, Idaho) was used as the non-reactive matrix to evaluate the effect of probe sampling on the matrix and probe performance. This silica is a non-reactive low alkaline oxide matrix with a characterized particle size distribution (Table S1), thus allowing absolute concentration measurements of the control gases

2.1.3 Gas sampling system

The soil probe sampling system operated in a continuous flow mode. In this approach, for each sample measurement we flowed carrier gas through the soil probe to equilibrate with soil gas (probe flow), then diluted the outflow online (dilution flow) and sent the combined flow (total flow) to the gas analyzer for real time measurement. The gas sampling system consisted of the following components: custom gas control, probe sampling, and a measurement and data acquisition system that integrated three gas columns (Fig. 2). Similar sampling systems were built at UA (System 1) and Aerodyne (System 2) and differed in the specific TILDAS and gas control components deployed at each location (Table 2). In order to prevent bulk gas advection in the soil it was critical to ensure that flow into and out of the probe were matched such that probe + dilution = instrument intake. As such, system control and sampling depended on precise flow control by digital mass flow controllers (MFC, Alicat Scientific, Tucson, AZ, USA). Dilution flow was important in the system (Fig. 2) to reduce risk of condensation, avoid exceeding optimal detection range, and increase gas analyzer cell response time. The control gas system allowed us to stipulate the specific mole fractions and relative isotope mixtures at the column inlet. Custom control gas composition was mixed from Ultra Zero Air (UZA; Airgas Inc.) and concentrated gas cylinders (e.g. 5% CO_2; Table 3). A bypass line was installed to independently verify the control gas composition entering the column while the column outflow line was used to measure column headspace concentrations (Fig. 2). A needle valve was added to the bypass line in System 2 to address inconsistent dilution rates observed in the control gas bypass line of System 1 (Fig. 2). We used UZA as the probe sampling carrier gas. Two streams of UZA controlled by MFCs were delivered in tandem through a stream selector 16x2 port valve (VICI Valco Instruments Inc. Houston, TX, USA) to the probe inlet (probe flow) and a PEEK “tee” connection at the probe outlet for dilution flow. The latter diluted the probe gas stream, with the total flow directed to the analyzer (Fig. 2). A second stream multiport selector (VICI Valco Instruments Inc. Houston, TX, USA) was used to select the resultant total flow to deliver to the analyzers.

We integrated multiple columns with the TILDAS using an automated multi-valve system. In System 1, we used a custom LabVIEW (National Instruments, Austin, TX) program to precisely execute scripts generated in Matlab (The MathWorks Inc.; 2018. Natick, Massachusetts) for timing and control of MFC gas flow rates and VICI valve switching. The LabVIEW program queried and logged MFC parameters and SDI-12 via USB multi-drop box (BB9-RS232, Alicat Scientific,

https://doi.org/10.5194/bg-2020-401
Preprint. Discussion started: 28 December 2020

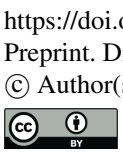

Tucson, AZ, USA) interfaces. In System 2, TDLWintel, the TILDAS measurement and data acquisition program, controlled the multi-valves on a schedule for continuous unattended operation.

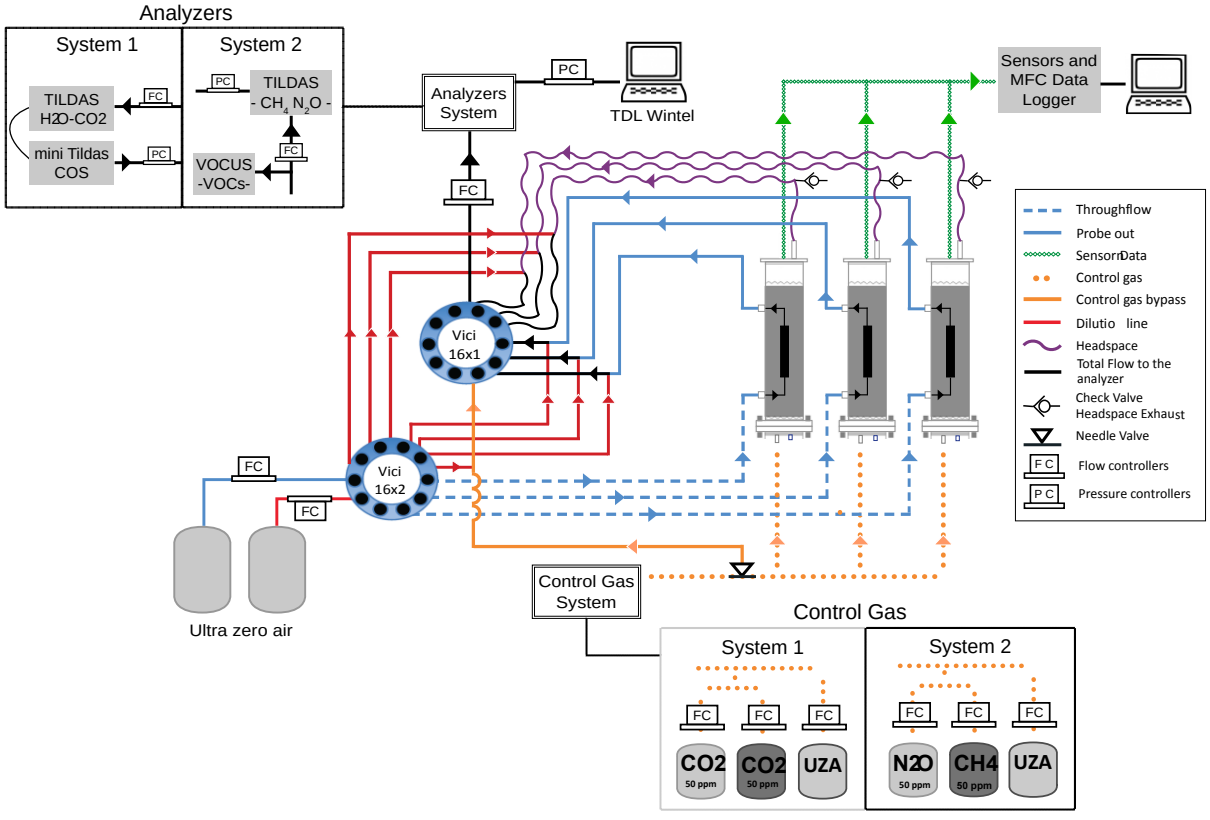

Figure 2. Detailed schematic of sampling System 1 (UA) and System 2 (ARI). Column matrix gas concentrations were controlled by mixing cylinder gas with UZA using MFCs and delivering the custom gas mixture through the columns from bottom to top (orange dotted line). Probe sampling flow rates were controlled precisely using three MFCs to ensure that flow in and out of the probe was balanced (*sample flow* (blue lines) + *dilution flow* (red lines) = *total flow to analyzer* (black lines)). Column headspace (atmospheric pressure) and control gas bypass (positive pressure) were controlled by MFCs at two points (*dilution*, *total flow to analyzer*), forcing the *sample flow* as a makeup flow (*sample flow* = *total flow* – *dilution flow*).

https://doi.org/10.5194/bg-2020-401
Preprint. Discussion started: 28 December 2020

Biogeosciences Discussions Open Access EGU

Table 2. Contrasting features between Systems 1 and 2

Feature	System 1	System 2
Objective	Feasibility of probe-TILDAS integration	Versatility of soil gas probe sampling
Location	Biosphere 2, University of Arizona, Tucson, AZ	Aerodyne Research Inc., Billerica, MA
Analyzer 1	Dual-laser TILDAS for H_2O and CO_2 isotopes	Novel dual-laser TILDAS for N_2O and CH_4 isotopes
Analyzer 2	Mini TILDAS for OCS, CO, CO_2, and H_2O	Vocus PTR-T OF-MS for VOCs
Control Gas (bulk)	Ultra-Zero Air	Ultra-Zero Air; Ultra-High Purity N_2
Control Gas (trace)	5% CO_2 in air	49.1 ppm N_2O in air; 54.6 ppm CH_4 in air
Flow Control	0.6 to 1 SLPM per column	0.65 SLPM per column
Matrix	Silica	Silica, Soil

To evaluate the probe and the column performance, we corrected observed concentrations (C_{obs}) using the ratio of the dilution and total flows to obtain true probe sample, column/headspace, and control gas concentrations (C). For example Eq (1), for soil probe sample concentrations we used the ratio of the total flow (F_t; probe sample plus dilution flow) to the probe sample flow (F_p):

$$C = C_{obs} * F_t / F_p \quad (1)$$

2.2 Trace gas analyzers

To characterize soil probe performance, we used a suite of trace gas analyzers relevant to biological soil gas cycling (Fig. 2). The system and analyzers were modified as needed to integrate with the soil probe sampling system. TILDAS isotope analyzers measure the concentrations of individual isotopologues, and isotopic ratios can be determined using Eq. (2),

$$\delta^i X = (R_n / R_{reference} - 1) \times 1000 \quad (2)$$

where, R_n refers to the ratio of the rare isotopomer, ^iX, to its abundant isotopomer (Toyoda et al., 2017).

https://doi.org/10.5194/bg-2020-401
Preprint. Discussion started: 28 December 2020

2.2.1 Coupled laser spectrometers for CO_2 and H_2O isotopes and COS and CO

System 1 integrated two TILDAS trace gas analyzers (Aerodyne Research, Inc., Billerica, MA, USA) with the soil probe testing system to evaluate the feasibility of coupling the sintered PTFE probes with analyzers and evaluate performance under controlled conditions. TILDAS-1 was a dual-laser instrument configured for measurement of $^{1}H^{16}O^{1}H$, $^{1}H^{16}O^{2}H$, and $^{1}H^{18}O^{1}H$ at 3765 cm^{-1} and $^{12}C^{16}O^{16}O$, $^{13}C^{16}O^{16}O$, $^{12}C^{16}O^{17}O$, $^{12}C^{16}O^{18}O$ O at 2310 cm^{-1} with a 18 m absorption cell. TILDAS-2 was a compact single-laser instrument configured to quantify carbonyl sulfide (OCS), carbon monoxide (CO), water (H_2O), and CO_2 at 2050.4-2051.3 cm^{-1} with a 76 m absorption cell. The dual and Mini TILDAS analyzers had a 500 cm^3 and 300 cm^3 sample cell volume, respectively. The platform draws air samples through an absorption cell at low pressure where laser light is transmitted in a multi-pass configuration for long effective absorption path lengths. The laser is scanned at kilohertz rates over the rovibrational absorptions of the molecule(s) of interest. Transient light absorptions were fit to known Voigt profiles to determine molecular concentrations on-the-fly using Aerodyne's proprietary acquisition and analysis software, TDLWintel. For this experiment we connected the two TILDAS analyzers at controlled flow rate (500-250 sccm, MC-1SLPM-D, Alicat) in series, and cell pressure was dynamically controlled to 40 Torr (PCSC-EXTSEN-D-15C/5P, Alicat) between the two analyzer sample cells and vacuum pump (MPU2134-N920-2.08, KNF Neuberger, Trenton, NJ). The TILDAS optical tables were each purged with 100 sccm zero air.

In System 1, CO_2 concentrations varied linearly with controlled dilutions of 10% CO_2 tanks (Fig. S1 dual CO_2 cal), and absolute CO_2 concentrations were calibrated with a linear curve. We calibrated the $\delta^{13}C$-CO_2 from the concentration dependent relationship of $\delta^{13}C$-CO_2 vs observed [CO_2] (Fig. S2); specifically, we fit a gaussian equation to the relationship between ($\delta^{13}C$-CO_2 observed - $\delta^{13}C$-CO_2 true ~ -39.2 ‰ vs Vienna PeeDee Belemnite (VPDB)) and CO_2 concentration (accounting for standard deviation in $\delta^{13}C$-CO_2 measurements). We applied this CO_2-dependent correction to all $\delta^{13}C$-CO_2 values reported here.

2.2.2 Novel laser spectrometer for N_2O and CH_4 isotopomers

System 2 integrated a second and nearly identical (Table 2) gas sampling system with a novel dual TILDAS analyzer for isotopomers of methane (CH_4) and nitrous oxide (NO_2) (Aerodyne Research, Inc., Billerica, MA, USA) to test instrument modifications that help integrate soil gas sampling probes with laser spectrometry and demonstrate the versatility of soil probe gas sampling.

In this study, we identified and selected the best spectral region and laser technology for continuous high precision measurements of isotopomers of CH_4 ($^{12}CH_4$ and $^{13}CH_4$), and N_2O ($^{14}N^{14}N^{16}O$ ("446"), $^{14}N^{15}N^{16}O$ ("456"), $^{15}N^{14}N^{16}O$ ("546"), and $^{14}N^{14}N^{18}O$ ("448")). The regions near 2196 cm^{-1} (4.56 µm) and 1295 cm^{-1} (7.72 µm) provide interference-free measurements of N_2O and CH_4, respectively, and their rare isotopes. The 2196 cm^{-1} region is also capable of measuring CO_2 at soil-relevant concentrations (parts-per-thousand levels). The CH_4 and N_2O TILDAS system was optimized with respect to optical alignment, laser operating parameters (i.e. scan length, laser current and temperature settings), and fit parameters.

https://doi.org/10.5194/bg-2020-401
Preprint. Discussion started: 28 December 2020

Short- (seconds) and long-term (minutes-hours) noise were determined by sampling from a compressed air cylinder as a constant gas source, followed by Allan-Werle variance analysis (Werle et al., 1993). We chose 30 Torr as the optimum cell pressure to minimize both noise and spectral crosstalk between isotopomer absorptions. To reduce sample volume we designed a new cell insert and a compact 76 m pathlength multipass sampling cell. The novel volume-reducing insert for the 76 m cell has interior walls that match the contour of the multipass pattern and was 3D-printed using PA2200 nylon. After printing, the interior and exterior surfaces of the insert were sealed with urushi lacquer—a stable, durable, inert lacquer (McSharry et al., 2007). The turnover time of the cell volume with insert was evaluated in continuous sampling mode.

The concentration dependence of isotope δ values derived from infrared isotopic measurements is an analytical challenge that is instrument dependent. To minimize the concentration dependence we used: (i) frequent backgrounds to minimize offsets (i.e. immediately prior to each sample measurement), and (ii) identified best fitting parameters for each spectral region and application. During System 2 operation, we automated script schedules using an external command language (ECL) within TDLWintel that ran backgrounds, calibrations, and controlled valves.

Alcohols (e.g. methanol and ethanol) have weak features in the methane spectral window (1295 cm^{-1}), at levels typically below that of the isotopic precision. We tested whether VOCs would cause infrared spectral interferences with TILDAS analysis by exposing the instrument to artificially elevated part-per-thousand levels of methanol, ethanol, and formaldehyde—three species that may be common in soil. We found potential for interference near the $^{13}CH_4$ absorption at elevated alcohol levels, but did not observe this interference in the spectra collected from probes in the soil tested.

The System 2 calibration system used online mass flow control to dilute concentrated N_2O or CH_4 calibration gases into UZA. We used pure samples of N_2O from Massachusetts Institute of Technology (MIT Ref I and Ref II). The isotopic ratios of N_2O were determined by Isotope Ratio Mass Spectrometry (IRMS) and TILDAS measurements, and externally verified by *S. Toyoda* at Tokyo Institute of Technology (McClellan, 2018). For calibration of the soil matrix tests discussed below, we used MIT Ref II to make a surveillance standard of 1,000 ppm N_2O. After calibrating N_2O isotopes against the reference gas, observed lab air N_2O isotopic ratios were within 3‰ of the relatively stable isotopic ratios of ambient tropospheric N_2O (Snider et al., 2015): bulk ^{15}N value of 6.3-6.7‰, and site preference of 18.7‰ (Mohn et al., 2014), and ^{18}O value of 44.4‰ (Snider et al., 2015). For CH_4 concentrations, a CH_4 surveillance tank served as a stable isotopic source to identify changes in isotopic composition.

2.2.3 High resolution volatile organic compound gas analyzer

In System 2 experiments, we integrated a Vocus PTR-TOF-MS (Aerodyne Research Inc., Billerica, MA, USA) (Krechmer et al., 2018) into the sampling system in parallel with the N_2O/CH_4 TILDAS, to detect soil VOCs such as monoterpenes, isoprene, and pyruvic acid (Gonzalez-Meler et al. 2014; Guenther et al. 1995). The Vocus technology contains a corona discharge reagent-ion source and focusing ion molecule reactor (fIMR) that has low limits of detection (less than part per trillion by volume) and fast time response, acquiring the entire mass-to-charge spectrum on the order of microseconds. A

https://doi.org/10.5194/bg-2020-401
Preprint. Discussion started: 28 December 2020

TOF instrument also has high resolving power in the mass dimension, enabling separation of isobaric signals (occurring at the same nominal mass-to-charge ratio). The TOF employed in this work consisted of a 1.2 m flight tube enabling a resolving power > 10000 m/dm. A sample flow of 100 SCCM was injected continuously into the Vocus source, with no extra overblow or carrier flow in the inlet line.

Data was processed using the Tofware (Aerodyne/TOFWERK A.G.) software package in Igor Pro (Wavemetrics). For these experiments PTR-TOF-MS was not quantitatively calibrated for the signals reported below, as we were only interested in relative concentration responses to wetting. Thus, signals are reported in non-normalized counts/s (Hz).

2.3 Experiments performed

We performed experiments using Systems 1 and 2 (Section 2.2; Fig. 2) to demonstrate the feasibility and versatility in coupling the permeable soil gas probes to trace gas analyzers to measure in situ gas concentrations and isotope ratios in soils. We conducted two categories of experiments: 1) *Experiments under controlled conditions using silica*, characterizing the ability of probe sampling to measure known, controlled soil gas concentrations; and 2) *Experiments with soil*, characterizing the ability of probes to capture soil microbial gas cycling dynamics from natural soils in response to environmental changes.

2.3.1 Experiments under controlled conditions using silica

Silica sand was used to limit trace gas production or consumption from the matrix for controlled evaluation of the probe. Three columns with one soil gas probe each were filled with dry silica matrix (Table S1) and closed hermetically. Gas concentrations and isotopic signatures of the inlet, soil probe, and column headspace samples were quantified while the gases flowed continuously through the column and dilutions rates were varied (Table 3).

We evaluated the *effect of probe sampling on the column* (Experiment 1) by changing the probe flow rate with constant control gas concentration and dilution. With System 1 and a single column with silica matrix, we alternated measurement of CO_2 concentration in headspace gas (1 h) and the probe (15 min) to determine the impact of probe sampling on soil column outflow concentrations. Next, we tested the flow conditions that support the probe delivering fully equilibrated and representative samples by *varying flow and dilution* at constant column concentrations (Experiment 2). We evaluated 42 combinations of set points for total flow (from 50 to 300 sccm, at 50 sccm intervals) and dilution (from 90% to 9%, at 15% intervals). Each measurement cycle lasted 25 min (15 min probe; 10 min column headspace) using one probe in System 1 and System 2.

We scaled-up the sampling systems to 3 probes to evaluate multiple online probe sampling (Experiment 3). We measured probe and headspace gas at a constant dilution (75%) of a 2000 ppm CO_2 control gas for a target observation concentration of 500 ppm and probe flow rates of 5, 10, 20, 30, 40, 50, and 100 sccm (System 1). System 2 was similarly evaluated with N_2O and CH_4 control gases in the silica matrix (Table 3).

https://doi.org/10.5194/bg-2020-401
Preprint. Discussion started: 28 December 2020

312 **Table 3.** Experiments under controlled conditions with silica matrix using Systems 1 and 2

Experiment	Columns	Probe Pore Size (µm)	Total flow (sccm); Probe Flow (sccm); Dilution (%)	Control gas (ppm)	System
1. Effect of probe sampling (silica)[a]	1	P8 (8 um)	total (10-600); probe (5-300); dilution (50%)	CO_2 1000	1
2. Flow and dilution[a]	1	P8 (8 um)	total (50:50:300); probe (0-300); dilution (90:15:0%)	CO_2 1000	1, 2
3. Multi-probe evaluation[a]	1	P8 (8 um)	total (20-400); probe (5-100); dilution (75%)	CO_2 2000	1
	2	P10 (10 um)			
	3	P5 (5 um)			
	4	P8 (8 um)	total (250); probe (25); dilution (90%)	N_2O 3ppm CH_4 7 ppm	2
	5	P10 (10 um)			

313 [a] Experiments 1-3 were conducted with the column top closed and no water addition.

314 **2.3.2 Experiments with soil**

315 We replaced the silica matrix with soil in the columns to understand probe behavior and response when monitoring
316 soil gases in a complex and dynamic soil matrix. We measured N_2O and CH_4 concentrations and isotopic signatures with the
317 improved TILDAS instrument on System 2 (Fig. 2) in a series of experiments (Table 4). For soil experiments, headspace
318 measurements can be used to track surface gas fluxes, but do not represent control gas concentrations as in the silica
319 experiments. We evaluated how measured soil gas concentrations changed in response to: probe sample flow rate (Experiment
320 4); environmental manipulations to the soil matrix (e.g. increased soil moisture with 5.1 cm of simulated rainfall) (Experiment
321 5); and forced changes to soil redox state (e.g. forced N_2 and UZA through the columns to shift from anaerobic to aerobic soil
322 environments) (Experiment 6). In this last experiment, we integrated the Vocus PTR-TOF-MS to the system to measure soil
323 VOCs (Fig. 2).

https://doi.org/10.5194/bg-2020-401
Preprint. Discussion started: 28 December 2020

Table 4. Experiments under controlled conditions with soil and silica matrix using System 2

Experiment	Type of soil	Columns	Probe	Total flow (sccm); Probe Flow (sccm); Dilution (%)	Control N_2O; CH_4 (ppm)	Soil Moisture
4. Soil vs. silica: multi-probe flow rate dependence	Soil 1	4	P8 (8 um)	total (235); probe (60); dilution (74%)	N_2O 3 ppm; CH_4 7 ppm	Field moisture
	Silica	5	P10 (10 um)			Dry
	Silica	6	P25 (25 um)			Dry
5. Soil wetting[a]	Soil 1	4	P8 (8 um)	total (50-100); probe (25); dilution (50-75%)		Dry to wet
6. Soil redox: anaerobic (N_2) to aerobic (UZA)[ab]	Soil 3	5	P10 (10 um)	total (185); probe (53); dilution (71%)		Wet

[a] Experiment conducted with the column top open

[b] Experiment integrated Vocus PTR-TOF-MS for VOCs

2.4 Data processing

For System 1, we used RStudio and R version 3.3.2 (Team, 2017) to integrate raw with metadata. Igor Pro (version 7, WaveMetrics, Lake Oswego, OR) for System 1 and System 2 was used to analyze instrument diagnostic, concentrations and times series. We averaged the last 80% to 90% of each measurement. Measurements were dilution corrected to obtain undiluted sample concentrations (Equation 1). In controlled tests when true headspace concentrations were measured before and after a probe measurement, these values were interpolated for comparison against probe concentrations to determine fractional recovery of soil gas concentrations.

3. Results and Discussion

3.1 Instrument improvement (N_2O/CH_4 isotopomer TILDAS)

3.1.1 Selection of spectral regions.

We selected optimal spectra windows and laser technologies for detection of the isotopomers of both CH_4 and N_2O using fundamental rovibrational transitions (Fig. 3). We used Aerodyne-developed simulation programs that utilize the HITRAN database (Rothman et al., 2013) to perform spectral simulations to identify potential measurement regions. Based on these simulations, we obtained appropriate lasers and detectors for the selected spectral regions. Simulations assumed an N_2O

https://doi.org/10.5194/bg-2020-401
Preprint. Discussion started: 28 December 2020

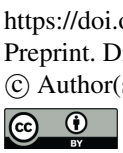

Biogeosciences Discussions Open Access EGU

mixing ratio of 1 ppm (parts per million, lower end of expected (Rock et al., 2007) in a mixture with 1.3% H_2O, 1% CO_2, 220 ppb CO and 1.9 ppm CH_4, at 30 Torr in a 76.4 m pathlength sample cell. This resulted in the selection of a spectral region (Fig. 3a) where all four N_2O isotopomers of interest, $^{14}N^{14}N^{16}O$ ("446"), $^{14}N^{15}N^{16}O$ ("456"), $^{15}N^{14}N^{16}O$ ("546"), and $^{14}N^{14}N^{18}O$ ("448"), have absorptions in close spectral proximity (<1 cm^{-1}), but without overlap of absorptions of each other or other trace gases such as from CO_2. The 2196 cm^{-1} region was used to monitor the N_2O isotopologues and CO_2 in the soil gas matrix using a quantum cascade laser (QCL) (Alpes Laser, Switzerland). We selected a second QCL (Alpes Laser) based on simulations of methane isotopes in the 1294 cm^{-1} region to monitor $^{12}CH_4$ and $^{13}CH_4$ isotopomers (Fig. 3b). This region also provided measurement of H_2O content in the soil gas via a water spectral feature at ~1294.0 cm^1.

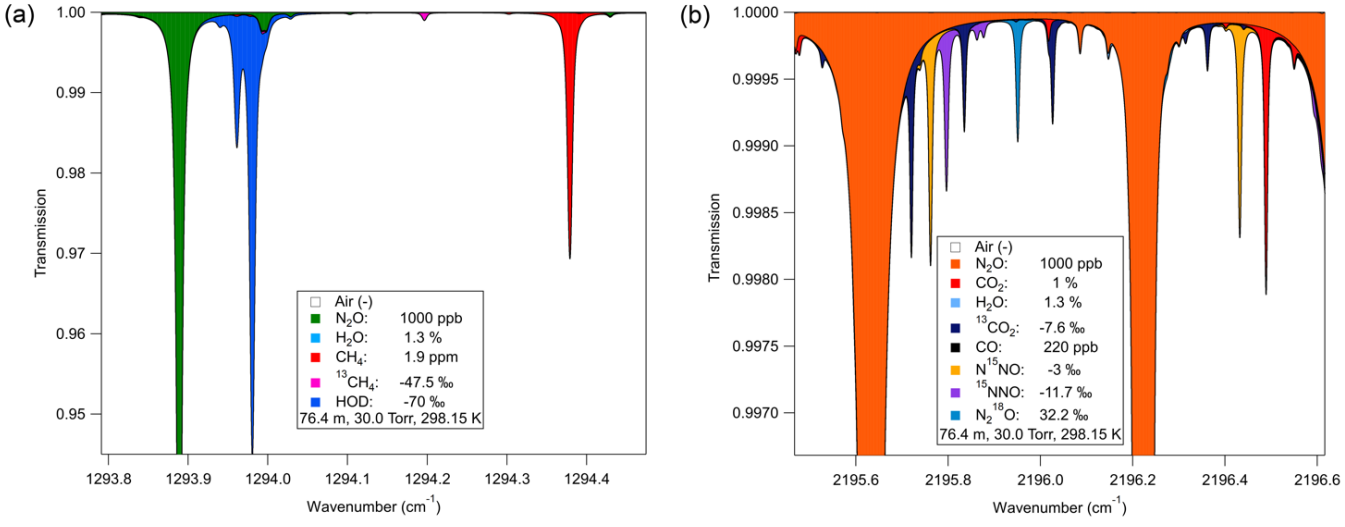

Figure 3. Isotopomers spectral regions for monitoring N_2O and CH_4 isotopomers. (a) N_2O isotopologue spectrum near 2196 cm^{-1}. Four N_2O isotopomers were present and spectrally separated, yellow and purple refer to the ^{15}N isotopomers with different positions relative to the oxygen. Blue refers to the ^{18}O isotopomer. (b) Spectral simulation of 1294 cm^{-1} region for methane analysis with lines well separated from H_2O and N_2O.

3.1.2 Optimization of isotope ratio measurements

TILDAS operational parameters were optimized to increase isotope ratio precision. For example, we monitored the slightly weaker doublet at 2196.2 cm^{-1} that had lower concentration dependence than the stronger absorber singlet at 2195.6 cm^{-1} that would produce nonlinear dependence at high mixing ratios. In addition, we modified fitting parameters to minimize impact of baseline variability on measurement precision (fit shown in Fig. S3). These improvements in spectral fitting helped minimize the dependency of N_2O and CH_4 isotopic ratios on concentration. Specifically, we reduced the slope of δ vs mole fraction to 0.7 ‰ ppm^{-1} N_2O (for N_2O < 8 ppm) and 0.5 ‰ ppm^{-1} CH_4 (for CH_4 < 14 ppm). The online dilution approach was

https://doi.org/10.5194/bg-2020-401
Preprint. Discussion started: 28 December 2020

critical for avoiding N_2O and CH_4 concentrations in soil exceeding these linear ranges. We quantified the precision of the isotopic ratios (Table S2) using Allan-Werle plots (Werle et al., 1993) (Fig. S3).

3.1.3 Sample cell reduction

We improved measurement response time by reducing TILDAS sample cell volume while maintaining the spectroscopic path length. Unnecessary 'dead' volume in the sample cell was eliminated through two approaches. First, we reduced the cell volume (port to port) by 20% (610 cm^3 to 485 cm^3) by shortening the cell by 4.2 cm, eliminating dead volume behind the mirrors. Second, the insert reduced the cell volume by ~50% (485 to 245 cm^3) by filling volume between the mirrors, but in the region outside of the multi-pass laser path. Overall, these changes reduced cell volume from 610 cm^3 (previous ARI 76-m Astigmatic Multipass Absorption Cell (AMAC) cell) to 245 cm^3, which improved the cell response time by 40%, here defined as the time to observe 75% of a full transition in concentration (Fig. S4) (i.e. from 1.13 (0.005)) s to 0.76 (0.01) s; 30 Torr and 1 SLPM). At the cell pressure of 30 Torr used here, this 245 cm^3 absorption cell volume corresponds to 9.7 cm^3 of sample gas at ambient pressure.

3.2 Probe performance under controlled conditions (silica sand)

3.2.1 Effect of probe sampling on soil gas concentrations (Experiment 1)

Soil probes sample subsurface gases by diffusion across the probe membrane into a UZA stream flowing through the probe. In our balanced mass flow approach, an equal proportion of UZA molecules diffuse out of the probe relative to soil gas diffusing in, which can affect (i.e. dilute) concentrations in the subsurface environment. To quantify the impact of probe sampling on soil column concentrations, we set control gas to 1000 ppm CO_2 and varied the probe flow rate from 5 to 300 sccm, and back, at a constant dilution (50%). We evaluated the impact of a 15-min soil probe measurement on subsequent 1-hour measurements of the column headspace. We found that column CO_2 concentrations were depleted directly following probe sampling (from 0.6 to 1.6% depletion) and took > 1 hour to fully stabilize. Column CO_2 was most depleted after higher probe flow rates (Fig. 4) due to increased CO_2-free UZA diffusion through the probe membrane. Low probe flow rates helped minimize these sampling artifacts on subsurface concentrations.

https://doi.org/10.5194/bg-2020-401
Preprint. Discussion started: 28 December 2020

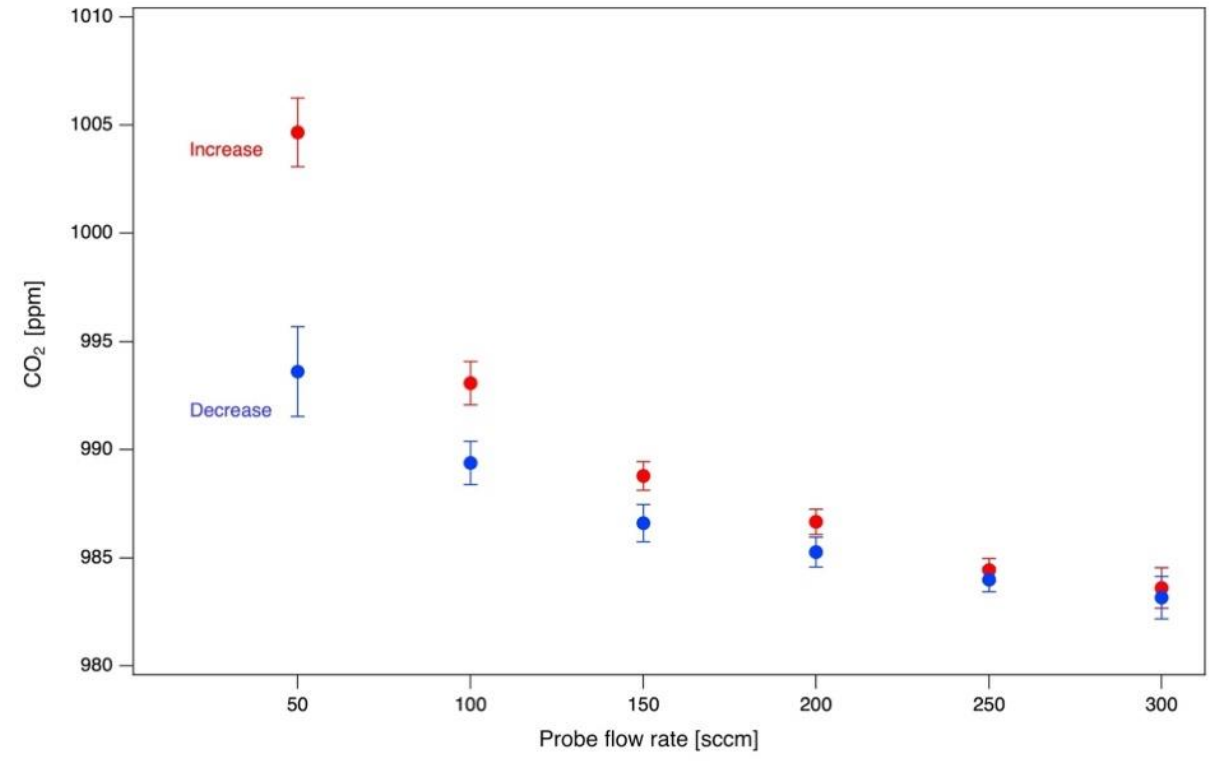

Figure 4. Effect of probe flow rate on column gas concentration (System 1 Dual). Points represent concentration of CO_2 in the headspace column for one hour after a 15-min probe sampling event at various increasing (forward) and decreasing (reverse) probe sampling flow rates.

3.2.2 Impact of probe flow rate and dilution (Experiment 2)

Compared to the controlled soil gas concentrations (Fig. 5), the probe-sampled concentrations were lower. When probe carrier gas is not flowing, the volume inside the probe is fully equilibrated with soil gas. This resulted in the observed initial 'pulse' of high gas concentrations when a probe was first selected and measured. During sampling, probe gas concentrations drop to a steady-state value that represents a balance between probe flow rate and the diffusion rate of soil gas molecules into the probe.

https://doi.org/10.5194/bg-2020-401
Preprint. Discussion started: 28 December 2020

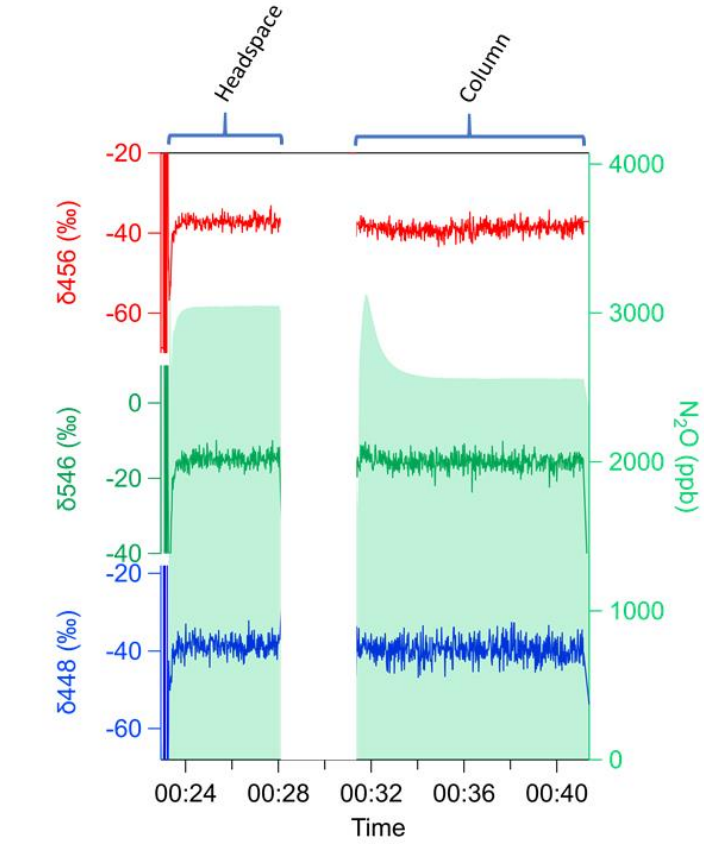

Figure 5. Headspace and probe measurements of N_2O using silica in System 2 (CH_4/N_2O). Example of initial pulse that equilibrates under flow-through and incomplete diffusion of N_2O concentration (green shade) with undetectable isotopic fractionation of isotopomers ☐456 (red), ☐546 (green), ☐448 (blue).

Gas samples obtained by probes at low probe flow rates were most representative of soil gas, as the slower flow rates allow more complete diffusive equilibration. We evaluated the impact of combinations of different total flow rates (from 50 to 300 sccm at 50 sccm increments) with sample dilution ratios (from 0 to 90% dilution at 15% increments) resulting in probe sampling flow rates between 5 and 300 sccm. These tests were conducted in the silica matrix with controlled soil gas composition (1000 ppm CO_2) (Experiment 2). We found that observed soil probe concentrations decreased with increases in probe flow rate (Fig. 6, Fig. 7), with no systematic influence of the dilution ratio. For the probe tested (Table 4), flow rates below 24.5 sccm produced representative samples (within 90% of true concentration). We did not observe any clear drawbacks to sampling CO_2 at flow rates <50 sccm (Fig. 7).

https://doi.org/10.5194/bg-2020-401
Preprint. Discussion started: 28 December 2020

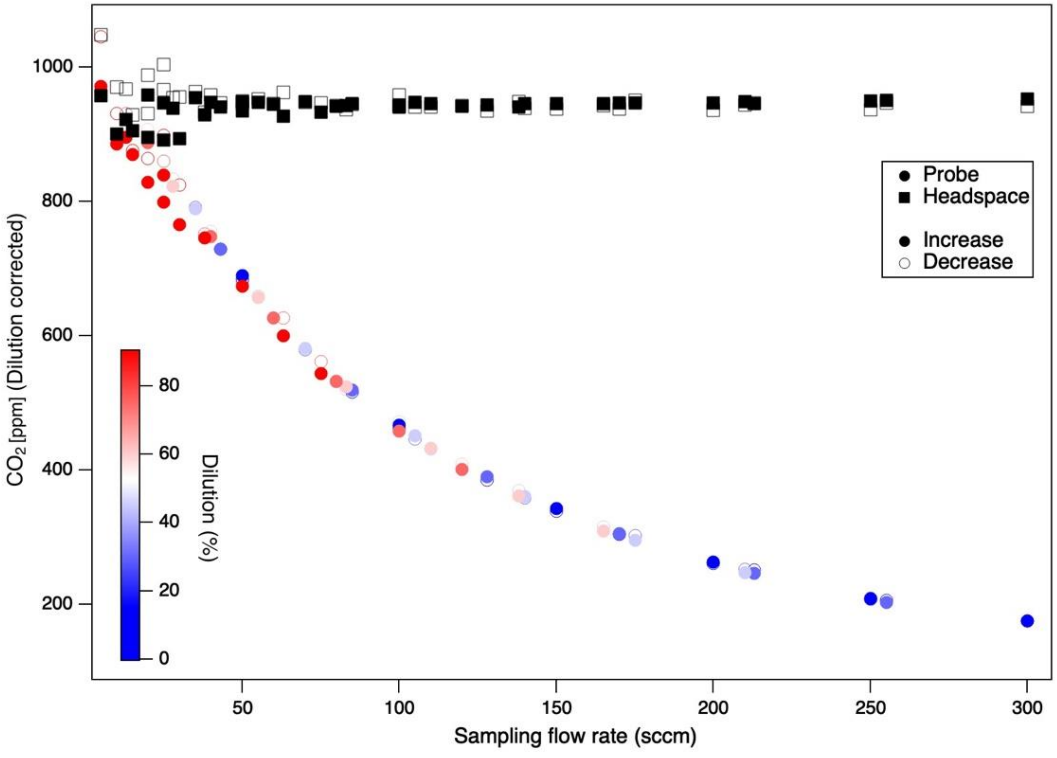

Figure 6. Probe and headspace CO_2 over a range of probe flow rates and dilution ratios (color). Column soil gas concentrations (headspace) remained steady across the experiment, while gas concentrations sampled by the probe diverged from true values at high probe sampling flow rates. Similar patterns were observed for independent experiments run with the reverse sequence from low to high *vs.* high to low probe flow rates (open vs closed symbols). CO_2 concentrations are dilution corrected (System 1 Dual).

Probe flow rates affected gases unequally, and based on their diffusivity. Probe recovery was lower for CO_2 with lower diffusivity than CO (molecular diffusion coefficients in air at 20°C: (CO_2 0.14, CO 0.18) (Bzowski et al., 1990; Massman, 1998) (Fig. 7). The fractional recovery of true soil gas concentrations by probe gas sampling (i.e. probe:column headspace ratios) was higher (0.65) for CO than CO_2 (0.2) at high flow rates (300 sccm). Additionally, the recovery ratios at specific flow rates were more scattered at a higher flow rate for CO. Regardless of the diffusion coefficient, both CO_2 and CO reached equilibrium at low probe flow rates, but CO was well-equilibrated over a 4x wider range (5-100 sccm) than CO_2 (5-25 sccm). Moreover, for molecular isotopologues (e.g. $^{12}CO_2$ vs $^{13}CO_2$), at increasing probe flow rates, the sampled CO_2 □^{13}C appears to be lighter than the headspace control by ~ -6 ‰ (Fig. 8) at the highest probe flow rates; showing that with incomplete equilibration, lighter isotopologues with higher diffusivity preferentially diffuse into the probe (here $^{12}CO_2$ vs $^{13}CO_2$). That this fractionation was observed relative to the headspace measurements implies it is derived from the probe, rather than the

https://doi.org/10.5194/bg-2020-401
Preprint. Discussion started: 28 December 2020

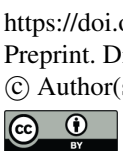

418 rest of the sampling system (tubing, multiport valves, MFCs). These concentration and isotopic fractionation results underscore
419 the need to ensure that the probe flow rate is sufficiently low to ensure full diffusive exchange between zero air and soil gas
420 before the gas sample exits the probe.

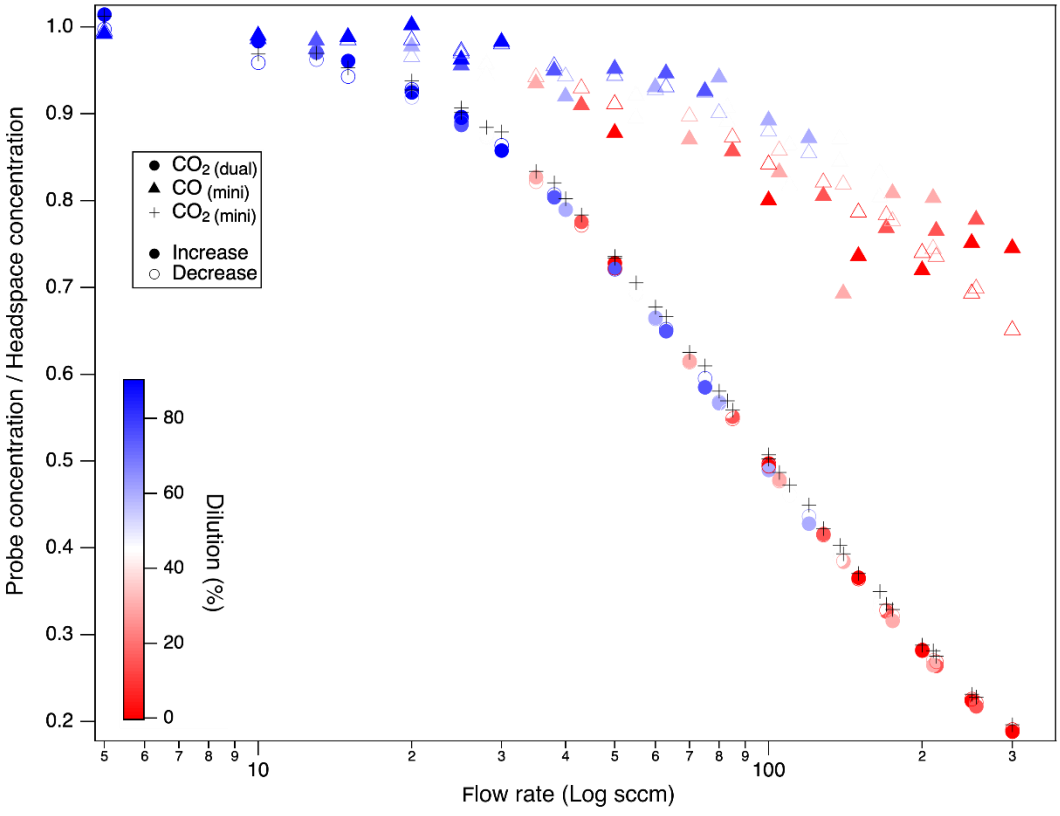

421 **Figure 7.** Impact of probe sampling flow rate on the fractional recovery of true gas concentrations by probe gas sampling for
422 trace gases with differing diffusivity (CO > CO_2) respectively, represented as the fractional recovery (probe:headspace
423 concentration ratio) during a test with a sequential increase in probe flow rate (forward in filled symbols) followed by a test
424 decreasing (reverse in open symbols) the flow rates. Dilution corrected CO_2 and CO on System 1 Mini and Dual TILDAS.

https://doi.org/10.5194/bg-2020-401
Preprint. Discussion started: 28 December 2020

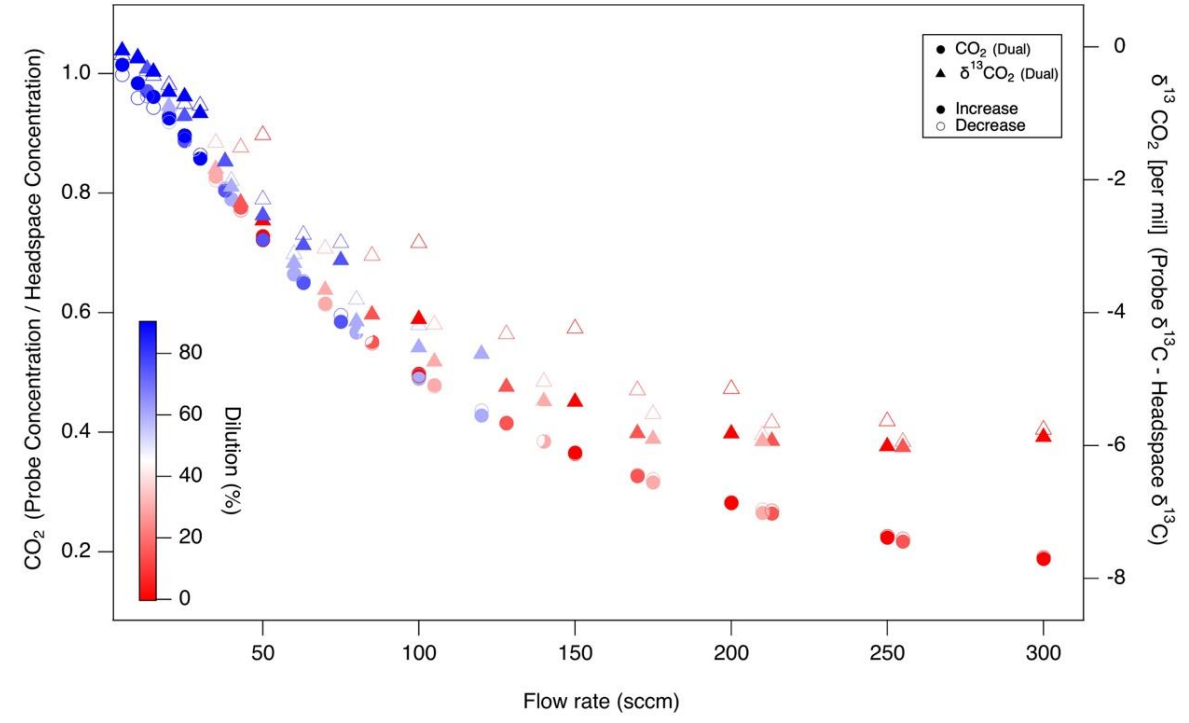

425 **Figure 8**. Impact of probe sampling flow rate on the fractional recovery of true CO_2 concentrations (left axis, circles) and the
426 offset in true soil □^{13}C (right axis, triangles) by probe gas sampling. As in Fig. 7, sequential probe flow rate increases (filled
427 symbols) and decreases (open symbols) tests plotted together. Dilution corrected in System 1 Dual.

428 **3.2.3 Demonstration with multiple probes (Experiment 3)**

429 We up-scaled the online diffusive probe sampling method in both System 1 and 2 to automatically control multiple
430 probes using lower flow rates (<100 sccm) to measure soil gas concentrations and isotopic ratios (Figure E). To fully constrain
431 probe measurements in the silica matrix (Table 3), each probe was evaluated repeatedly over a full sampling cycle (~25
432 minutes) to measure headspace-probe-headspace. In both systems, we could scale to sequential measurements of multiple
433 probes with good sample recovery (e.g. minimal concentration loss, isotope fractionation). In particular, probe recovery of
434 N_2O isotopomers was within 3‰ from true headspace values, and equilibration of all trace gas species generally was near or
435 above 85% (Fig. 9). Multiprobe tests showed that the system has a high potential for scalable spatial resolution and scalability.
436

https://doi.org/10.5194/bg-2020-401
Preprint. Discussion started: 28 December 2020

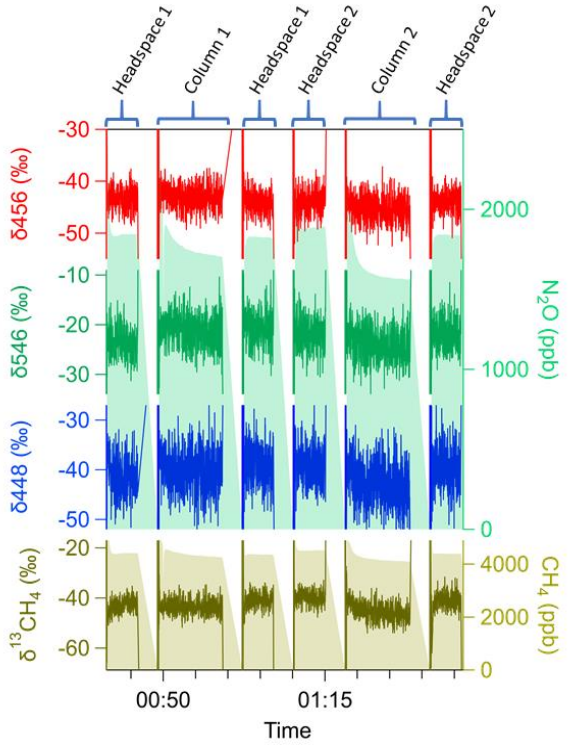

Figure 9. Soil probe sampling approach up-scaled to multiple probes (System 2). Multiprobe tests measured headspace-probe-headspace sequentially for (top panels) N_2O (green shade; right side) including isotopic ratios for three N_2O isotopomers δ456 (red), δ546 (green), δ448 (blue) and (bottom panel) δ^{13}C-CH_4 (brown; left axis) and CH_4 (brown shade; right axis) in the left axis.

We used the multiprobe system to determine whether probes with different properties would exhibit the same flow dependency, and in particular, the effect of characteristic pore size of a sPTFE probe upon concentration recovery. The flow rate dependence of the different probes was determined with CO_2 in silica sand (Fig. 10). Our observations of probe flow rate dependency for one pore size (P1) predicted the general behavior of others (P2-P3) across a 5-10 µm pore size range. Unexpectedly, we did not find a clear link between the pore size and the fractional recovery of true soil CO_2 concentrations for any given flow rate. For example, we might expect that a pore size of 10 µm would permit greater diffusion and favor probe equilibration; instead, the 8 µm probe produced a more equilibrated sample than either the 5 µm or 10 µm (Fig. 10. Because the pore density of the different probes is unknown, we cannot infer the relationship between the diffusion properties of the probes and the characteristic pore size.

https://doi.org/10.5194/bg-2020-401
Preprint. Discussion started: 28 December 2020

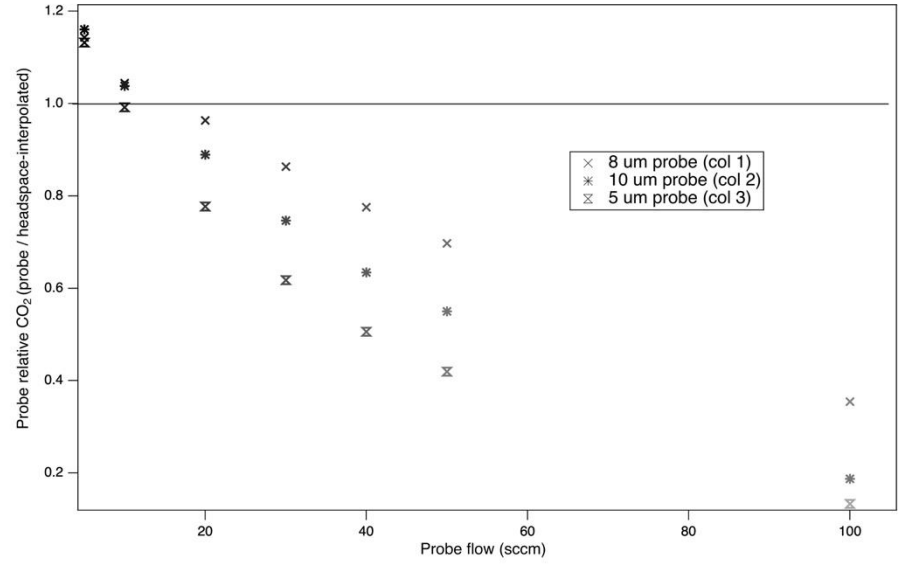

Figure 10. Impact of probe pore size on the relationship between probe sampling flow rate and fractional recovery of true soil gas concentrations. Multiprobe test with System 1 Dual. Each Column headspace-probe-headspace were measured sequentially, and headspace values were interpolated to calculate the fractional recovery.

3.3 Probe performance in soil

3.3.1 Impact of probe flow in soil vs silica (Experiment 3 and 4).

In System 2, at low probe flow rates the concentration measured from the probe was similar to the concentration in the headspace in the silica matrix. Probe flow rates above 25 sccm decreased probe concentration for both the 10 µm and 25 µm pore sizes (Fig. 11). Similar to Fig. 10, the fractional recovery did not increase with pore size, and we did not find that the 25 µm pore size transferred more gas into the carrier flow. In tests at higher probe flow in the silica matrix, the fraction of CH_4 recovered in the probe was higher than for N_2O. This result was consistent with our results in Fig. 7 and the known molecular diffusion rates of N_2O and CH_4 through soil, 0.14 $cm^2\ s^{-1}$ and 0.19 $cm^2\ s^{-1}$, respectively (Wang et al., 2014). Thus CH_4 diffuses into the probe and replenishes the area around the probe more quickly during sampling than N_2O.

In System 2, even in soil where controlled soil gas conditions were lacking (i.e. cannot constrain with headspace measurement), we observed a decline in measured soil gas concentrations with flow rate, similar to the silica matrix experiments (Table 3). The consistency in patterns across systems and soil matrix (controlled silica vs uncontrolled soil) provided additional support for the trends observed in the above experiments. The experiments that follow did not attempt to control soil gas concentrations in real soil and focused on probe gas and not headspace concentrations. In the following tests, we manipulated key drivers of soil function (moisture and redox) to elicit responses in soil microbial processes and soil gas concentrations to discover the in situ soil gas dynamics newly observable with our novel soil gas probe sampling system.

https://doi.org/10.5194/bg-2020-401
Preprint. Discussion started: 28 December 2020

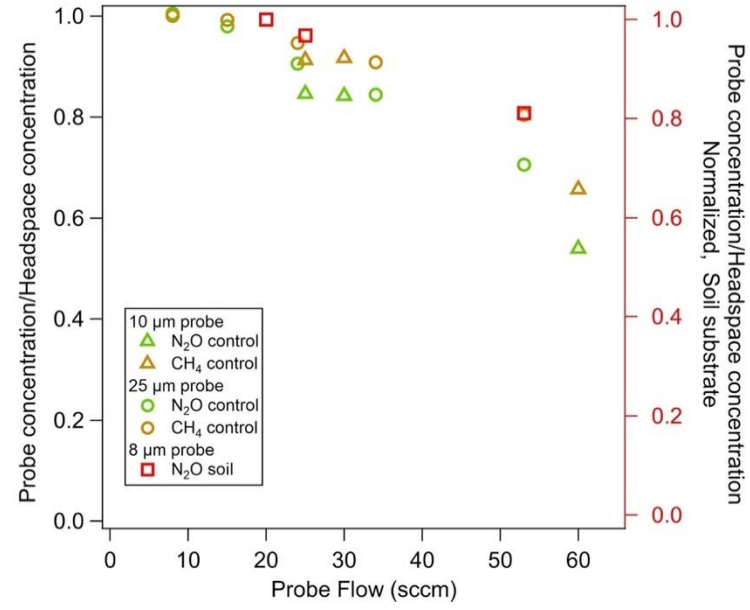

Figure 11. Impact of probe sampling flow rate, pore size, trace gas species, and soil matrix on the fractional recovery of true soil gas concentrations with probes. Fractional recovery of N_2O (green) and CH_4 (yellow) in a silica matrix with flowing control gas and probe pore size of 10 µm (triangle) and 25 µm (circles). The recovery of N_2O gas in soil at field moisture (red squares), normalized to high recovery, measured with probe pore size 8 µm. All measurements using System 2.

3.3.2 Soil dry-wet cycle (Experiment 5)

Soil wetting induced a strong pulse in subsurface N_2O concentrations, isotopic signatures, and site preference that was captured in detail with the N_2O and CH_4 TILDAS and real time in situ soil gas probe sampling. We found that the isotopic ratios of all three N_2O isotopomers (δ448, δ546, δ456), site preference, and N_2O concentration responded to the wetting over the subsequent 36-hour period. N_2O rose from approximately 3 ppm to over 40 ppm, with a corresponding and slightly delayed response in isotopic signatures (Fig. 12). The dramatic increase in N_2O required additional dilution at concentrations above the expected range of the TILDAS (>20 ppm). The response of the two ^{15}N-N2O isotopomers diverged enough to drive a shift in the site preference (SP) upward by approximately 4‰ to 6‰ before falling back down toward 2‰. After the peak, the decline in concentration and isotopic signatures was not explained by soil moisture, which was a relatively steady 25-30% volumetric water content (VWC) throughout the period. When mapped into a 3-dimensional isotope space (Fig. 12b) that is based upon previous observations of SP, $^{15}N_{bulk}$, and ^{18}O for a variety of different processes (Toyoda et al., 2017; Wei et al., 2019), the observed isotopic signature falls between chemodenitrification and bacterial denitrification. While the $^{15}N_{bulk}$, and ^{18}O signals are dependent upon the substrate ^{15}N and ^{18}O compositions, the shift over the course of the rewetting measurement indicates a period of more denitrification (at higher SP), then decreasing back to bacterial denitrification. Importantly, the

https://doi.org/10.5194/bg-2020-401
Preprint. Discussion started: 28 December 2020

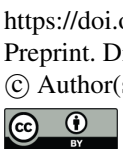

observed range of SP values is well below the expected range for bacterial and archaeal nitrification (AOB, AOA), which are >20 (off scale in Fig.12b).

In contrast to the dynamic response in N_2O, soil CH_4 concentrations remained low, leading to low signal-to-noise ratios in the detected ^{13}C-CH_4 isotopologue, and did not respond to wetting (data not shown). The dilution rate of the sample was increased by 1.9x at hour 18, resulting in a 1.9x reduction in N_2O concentration measured by the TILDAS (accounted for in Fig. 12). Despite the large change in concentration, the isotopic signatures barely changed, even after readjusting the dilution rate at hour 42, indicating that their concentration dependence had been well accounted for.

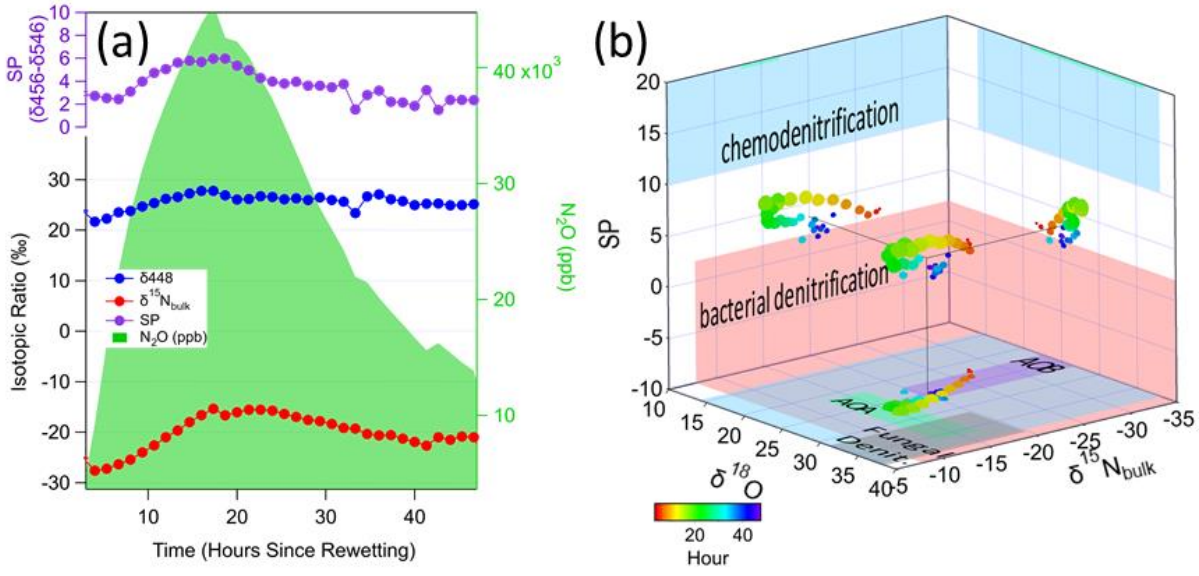

Figure 12. (a) Soil wetting induced a pulsed response in soil N_2O (shaded green) and its isotopic signals including δ448 (blue), δ546 (green), δ456 (red), and site preference (purple). A soil column without a lid was wetted with the equivalent of 5.1 cm of rainfall. At 18 hours after wetting the dilution was changed from 2:1 to 3.8:1, and at 41 hours it was changed to 2.1:1, which is accounted for in the concentrations reported here. **(b)** Estimated map of N_2O isotopic signatures of bulk $\delta^{15}N$ (x-axis), $\delta^{18}O$ (y-axis), and site preference (z-axis), circles represent probe measurements of the changes in the isotopic signatures with time (hours) indicating shifts into region of different microbial activity (colored rectangles) (Table S3). On the x-axis AOA (green rectangle) and AOB (purple rectangle) refer to nitrification from ammonia oxidizing archaea and ammonia oxidizing bacteria, respectively. Grey rectangle indicates fungal denitrification.

3.3.3 Soil responses to an anaerobic to aerobic shift (Experiment 6)

Shifting the soil redox environment from anaerobic to aerobic conditions induced a cascade of subsurface gas pulses in CO_2, N_2O, and VOCs that we measured by integrating TILDAS and Vocus analyzers with the real time in situ soil gas probe

https://doi.org/10.5194/bg-2020-401
Preprint. Discussion started: 28 December 2020

sampling. Before this experiment, the soil column was forced into anaerobic conditions by advectively flushing with N_2 through the control gas ports for 3.5 hours; subsequently, conditions were driven aerobic by flushing the system with UZA for a short time at time zero (Fig. 13). Conversion to aerobic conditions drove a pulse in N_2O concentrations that was slow and considerably weaker (reaching 1.6 ppm after 72 hours) than the wetting response (Experiment 5). The onset of aerobic conditions brought a strong CO_2 increase from 0.1 to 0.4%, suggesting an increase in microbial respiration. Along with CO_2 and N_2O, we measured a cascade of responses in masses corresponding to different VOCs. As respiration and nitrogen processing increase, the larger VOCs exhibit either immediate ($C_9H_{18}O$, $C_{11}H_{20}O$, e.g. nonanal, methylborneol) or delayed loss ($C_{10}H_{16}$ (monoterpenes), $C_{12}H_{22}O$, e.g. geosmin) in the soil. In contrast, after a few hour delay, the sulfur-containing compounds methanethiol (CH_4S) and dimethyl sulfide (CH_6SH) exhibited a surge in production. The approach captured different temporal responses to a shift in soil redox across a suite of soil gases that reflect different microbial processes and their sensitivity to environmental forcing.

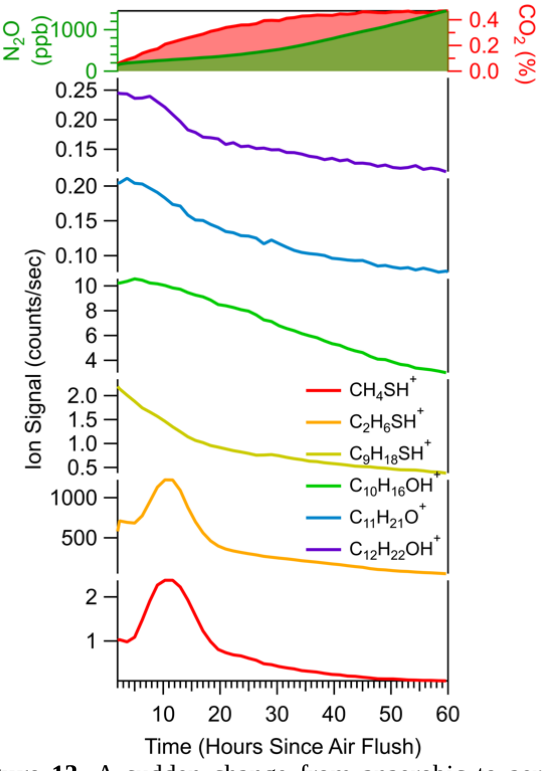

Figure 13. A sudden change from anaerobic to aerobic soil conditions, induced by flushing with UZA, drove dynamic responses in N_2O, CO_2, and a variety of VOCs captured using the diffusion-based soil probe integrated with the TILDAS and Vocus analyzers. System 2 Experiment 6 with a B2 TRF soil sample.

https://doi.org/10.5194/bg-2020-401
Preprint. Discussion started: 28 December 2020

4. Discussion

We developed a new soil gas sampling system that integrated diffusive sPTFE soil probes with a set of online and high resolution trace gas analyzers. The versatile system detected controlled and forced temporal changes in soil concentration and isotopic signatures of N_2O and CH_4 and VOCs.

4.1 Optimizing soil gas sampling

Optimizing soil gas sampling. Our results show that gas recovery depends on probe flow rate and the trace species, while the effect of dilution of the probe sample outflow on recovery is minimal. Probe flow rate determines the time available for carrier UZA to equilibrate with soil gas across the diffusive membrane as it flows through the probe: lower probe sampling flow rates allow more time to equilibrate than do high flow rates (Gut et al., 1998; Parent et al., 2013). By running tests in reverse order, we showed that the results were not dependent upon carry-over or memory effects. Correspondingly, we observed that the fractional recovery of true soil gas concentrations declined exponentially with increased probe flow rates across all systems (Fig. 8 and Fig. 11), analytes (Fig. 7), and probe characteristics tested. The maximum probe flow rates that delivered well-equilibrated samples (>90% equilibrated) ranged from ~25 to 100 sccm, depending on the system and, in particular, the molecule measured. Indeed, in both silica and soil matrix, gas recovery was better for molecules with relatively higher molecular diffusivity (i.e. CO, CH_4, ^{12}C-CO_2) than paired analysis of those with lower diffusivity (i.e. CO_2, N_2O, ^{13}C-CO_2) (Wang et al., 2014). Molecules with higher diffusivity move across the membrane and also replenish the area around the probe during sampling more quickly than those with lower diffusivity. As a result, the upper range of probe flow rates that produce representative gas samples will be higher for analytes with higher diffusivity, and more restricted for slow diffusing molecules. While isotopic fractionation was observed in some (CO_2; Fig. 8), but not all (N_2O; Fig. 9) tests, incomplete equilibration affected recovery of bulk concentration more strongly than isotopic signature, suggesting that optimized probe sampling can produce isotopically representative samples with minimal fractionation.

4.2 Factors yielding a representative sample

One of the challenges in soil trace gas measurements is transferring a representative sample (Parent et al., 2013) from probes to fill the relatively large sample cell volumes of online analyzers (e.g. 10s to 100s mL at reduced pressure). To address this issue, we reduced the effective volume of the TILDAS sample cell by designing a more compact cell with a volume-filling insert (Section 3.1). We also integrated online dilution into the sample transfer system after the probe, which increased the sample volume delivered to the sample cell without increasing probe flow rates. Dilution also helped reduce soil gas concentrations to within the range of sensitive trace gas analyzers and avoid condensation effects (none observed). Together, these modifications improved the transfer of representative soil gas samples to the cell, increased the turnover time of the cell leading to a faster time response, and supported lower probe flow rates facilitating probe equilibration (Jochheim et al., 2018).

https://doi.org/10.5194/bg-2020-401
Preprint. Discussion started: 28 December 2020

Beyond flow-through sampling, these modifications may be particularly important in future approaches that transfer equilibrated soil gas 'plugs' to an online analyzer for trapped-sample analysis. In addition, reducing sample demand also reduces the disruption of the soil probe measurement on the soil environment. The diffusive soil probes allow sample gas to diffuse into the probe from the soil environment, but also allow the UZA carrier gas to diffuse out of the probe into the soil. Under controlled soil conditions (silica and advective flow), probe sampling caused a < 2% decrease in soil CO_2 concentrations, with the impact decreasing at the low probe flow rates supported by our volume-reducing modifications. In real soil, the impact of carrier diffusion out of the probe could be larger where local gas concentrations are not replenished by advection but depend on local production, consumption, and diffusion. In addition to reducing sample volume, lowering the sampling frequency (return rate) may be especially important in real soil (Jochheim et al., 2018) helping to reduce the impact of the perturbation on the soil environment.

4.3 Transferability to multiple analyzers

The continuous online soil gas sampling approach is highly transferable across trace gases and instrument systems. Here, we successfully measured soil trace gases using two systems. Modifications to reduce sample volume requirements (i.e. online dilution, precise flow control, instrument modifications) are transferable to other analyzers beyond the N_2O/CH_4 isotopologues TILDAS. Although other laser absorption spectroscopy instruments like CRDS have been used to measure concentration and isotopic composition for trace gases like CO_2 (Voglar et al., 2019), TILDAS can measure several species at high sensitivity/spectral resolution with one instrument (McManus et al., 2015), are field deployable (McCalley et al., 2014; Roscioli et al., 2015; Saleska et al., 2006), and readily interface with the valving and flow control system designed here. Not only is the approach transferable across instruments, but we demonstrated that more than one instrument can be integrated for simultaneous soil probe sampling, e.g. Vocus PTR-TOF-MS for VOCs with the N_2O/CH_4 TILDAS in parallel (System 2), and two TILDAS in series (System 1). This versatility can be extended to allow analysis of a suite of soil gases using existing TILDAS technology to study, for example, soil microbial N cycling (e.g. N_2O, NO, NO_2, NH_3, HNO_3, HONO, NH_2OH), microbial trace gas scavenging (e.g. CO, OCS, CH_4, O_2), and other atmospherically-relevant species (e.g. H_2O_2, HONO, N_2H_4, HCHO, HCOOH, CH_3OH). These compounds represent metabolites for microbial communities, and intermediates of metabolic pathways of carbon and nitrogen cycling. Therefore, coupling these instruments with soil probes will enable access to previously unexplored biological information that reflects metabolic and signaling processes in the soil subsurface.

4.4 Capturing soil gas response to wetting

The optimized soil gas sampling system integrated with the novel N_2O/CH_4 TILDAS captured real time responses of subsurface N_2O isotopes to changes in soil moisture in soil column experiments. Soil wetting is a powerful and well-studied driver of biogeochemical change in soils known to result in a rapid release of soil gases such as N_2O (Birch effect) (Birch, 1958; Leitner et al., 2017). The soil probes, positioned at 20 cm below the soil surface, captured a significant increase in

https://doi.org/10.5194/bg-2020-401
Preprint. Discussion started: 28 December 2020

subsurface N_2O concentration almost immediately after water was added to the column, and a slow change in isotopic signature that suggests a more gradual change in the subsurface processing producing N_2O (Leitner et al., 2017; Van Haren et al., 2005). Our novel subsurface ^{15}N site preference measurements had SP signatures for N_2O production pathways between characteristic signatures suggested for bacterial denitrification and chemodenitrification pathways (Sutka et al., 2006; Toyoda et al., 2017). The rapid increase and slower decrease of N_2O suggest the initial pulse of microbial activity as a response to environmental changes can vary on long (days) and short timescales (minutes/hours) at this depth, both of which are recovered using this sampling system.

4.5 Capturing soil gas response to redox

The system displayed the potential to capture hotspots or hot moments of trace gas production, providing temporal information of key metabolic processes in carbon and nitrogen cycling. The introduction of UZA to change the redox status increased the abundance of microaerobic sites in soil stimulating heterotrophic respiration (CO_2 emissions). VOC production also responded to the changes in oxic and anoxic sites. VOCs are emitted as a byproduct of either respiration or fermentation processes as part of microbial metabolism in soil (Peñuelas et al., 2014). Small molecules and larger volatile organic compounds contribute to soil nutrient cycling, and therefore serve as valuable markers of different and highly specific microbial activity (Schulz-Bohm et al., 2015). For example geosmin and methylisoborneol are produced by actinomycetales (Citron et al., 2012; Peñuelas et al., 2014) under anaerobic conditions, while sulfurous VOCs are produced in micro-anaerobic sites in soil.

4.6 Implications for sPTFE as a field-based soil probe

sPTFE is known to exhibit hydrophobicity, chemical inertness, microfiltration properties, and uniform pore distribution (Dhanumalayan and Joshi, 2018). All sPTFE probes recovered representative soil gases, but without differences based on pore size. Sample recovery did not correlate with the characteristic pore size of the probes, and all sizes quantitatively recovered >90% of the analyte concentration at optimized flow rates. It is unknown whether the machining process modified the pore density of the surface of the probe; nevertheless, it did not damage the integrity or the resistance of the material, which preserved hydrophobicity and structure throughout the experiments. In >4 months of operation in laboratory soil, the performance of the sPTFE probes did not change with time or environmental conditions. In contrast, Panikov et al., 2007 found that the methane conversion factor for calibration using silicone membranes differed between a dry and wet membrane. (Rothfuss and Conrad, 1994) found memory effect issues when sampling high concentrations of CH_4 with silicone and epoxy as soil-gas exchange barriers. Soil probes made of polypropylene (PP) membranes have been widely used to measure CO_2 (Gut et al., 1998; Jochheim et al., 2018), and polyethylene (PE) for water isotopes in soils (Volkmann and Weiler 2014; Volkmann et al. 2018) and in tree xylem (Volkmann et al., 2016a). However, in our past experience (T. H. M. Volkmann, personal communication) PP and PE probes have shown decreased wall integrity during field deployment and long term use

https://doi.org/10.5194/bg-2020-401
Preprint. Discussion started: 28 December 2020

(i.e. dents and cracks) causing gas and water leaks, compromising hydrophobicity in saturated media. Our 15 cm probes are more rigid and smaller than previous probes that were typically 100 to 150 cm in length (Flechard et al., 2007; Gut et al., 1998; Parent et al., 2013; Rothfuss et al., 2013), and are easily installed via a small borehole. The sPTFE soil probes described here therefore have potential to be less disruptive to the soil ecosystem and more robust to soil structure and environmental changes for long-term measurements in the field.

4.7 Considerations for field deployment of the system

We show that diffusive soil probes can measure soil gases with cm-level spatial resolution for a time-dependent picture of the soil gas dynamics. This contrasts with other methods, e.g. manual sampling with syringe (Kammann et al., 2001) and cartridges (Wester-Larsen et al., 2020), that disturb the true soil gas concentration during sampling and also risk sample integrity during transfer for offline laboratory analysis (Volkmann and Weiler, 2014). Manual sampling also increases the potential measurement error, and is time consuming and labor intensive, particularly when attempting to sample at a high time resolution and/or to cover a large spatial area (Wester-Larsen et al., 2020). Our integrated sample system can achieve unattended, automated sequential and long-term field soil gas sampling that is less time consuming and less laborious.

In field implementation of our system, there are tradeoffs between sampling frequency and disruption that should be fully considered. As noted above, diffusive soil sampling can alter soil gas by dilution, and sample transfer parameters should be optimized to obtain representative samples with minimal disruption. This may be especially important for distant sampling points that require longer tubing that may release more zero air into the soil during sample transfer to the analyzer. The different modules of the sampling system (Fig. 2) are flexible and can be adjusted to accommodate multiple probes, different measurement specifications, and soil and environmental factors in the field.

5. Conclusion

Versatile trace gas sampling systems integrating soil probes and high resolution trace gas analyzers bridge an existing knowledge gap using in situ spatial (centimeter scale) and temporal (minutes) measurement of concentrations and isotopic signatures of soil trace gases. We demonstrated the feasibility and versatility of an automated multi-probe analysis system for soil gas measurements of isotopic ratios of nitrous oxide ($\delta^{18}O$, $\delta^{15}N$, and the ^{15}N site-preference of N_2O) and methane ($\delta^{13}C$), and VOCs, all important gas-phase indicators of biological activity. We present an experimental system to evaluate and optimize probe sampling under controlled conditions and demonstrate capabilities to resolve dynamic changes in real soil. The experimental approach captures snapshots of gas emissions as a result of changes in environmental drivers such as soil moisture and redox conditions, and observed hot moments showing the dynamics of microbial metabolism and communities. These tests demonstrate the potential of this approach to reveal interconnections between the soil microbiome and its local environment on timescales relevant to real-world variability.

https://doi.org/10.5194/bg-2020-401
Preprint. Discussion started: 28 December 2020

In order to keep expanding the usefulness of these probes, future work will focus on further characterization of probe material, pore size, and dimensions, with the goal of reducing size (and therefore sampling footprint) in order to access processes on smaller spatio-temporal scales. We will also explore probe assembly and installation approaches that minimize disturbance to the subsurface, and allow for rapid installation into soil.

The outlook is bright for integrating soil gas measurements with other data and models to unlock new understanding of soil microbial processes. Direct sampling of soil for subsequent laboratory incubations and analysis using multi-omic approaches is a sensitive and precise approach for identifying subsurface microbial populations and their potential metabolic function. Although both widely used approaches produce reliable and robust results, they are labor intensive and destructive, and incompatible with generating a well resolved spatial- and time-dependent understanding of microbial activity in natural ecosystems. Similarly, current soil gas sampling methodologies face challenges to address the gap between time-space sampling (e.g. frequency and intensity), low bias in downstream analysis, and proper reference materials. Isotopic signatures of trace soil gases, in conjunction with genomic and metabolomics approaches can elucidate real time biomarkers of microbial metabolisms in soil, leading to a better understanding of soil heterogeneity as a modulator of soil-microbe interactions and their responses to environmental factors and nutrient cycling. These efforts will help scale up soil trace gases monitoring and quantification of biogeochemical processes to improve modeling, soil management decisions, and soil health with high spatial and temporal resolution.

Data availability. Igor software was used under license. Igor scripts were used for data processing and analysis including Aerodyne Research Inc. proprietary scripts for parsing and averaging data and cannot be in a public repository. Other portions of Igor code used for plotting are available upon request. Raw measurements files (e.g., TILDAS and vocus spectra) will be available upon request. Processed data can be found at DOI: 10.25422/azu.data.13383014

Supplement. Additional supporting information available online at:

Author contribution. All authors made substantial contributions to the research. T.H.M.V, L.K.M., J.R.R., J.H.S. conceptualized the idea and acquired funding. All authors participated in part or all of developing prototypes, building experimental systems, and conducting experiments. J.G.L, L.K.M., J.R.R., J.H.S. contributed to the analyses and interpretation of data; J.G.L. and L.K.M. prepared the draft, all authors discussed the results and contributed to the final manuscript.

Acknowledgments. This material is based upon work supported by the U.S. Department of Energy, Office of Science, Office of The Small Business Innovation Research (SBIR) grant, Office of Science, under Award Number(s) DE-SC0018459. THMV was supported by Biosphere 2 through the office of the Senior Vice President for Research Innovation and Impact at the University of Arizona. We thank Doug White and White Industries, Inc. for machining the probes. The authors gratefully

671 acknowledge financial support from the Philecology Foundation for Biosphere 2 and the Landscape Evolutionary Observatory.
672 Prof. Shuhei Ono at the Massachusetts Institute of Technology has shared with us calibrated reference gases for this study.

673 **Conflicts of Interest.** Aerodyne Research Inc manufactures the TILDAS instrumentation and commercializes the Vocus PTR-
674 TOF for applications in geosciences. Probes, sampling systems and associated software are in development.

675 Disclaimer: *"This report was prepared as an account of work sponsored by an agency of the United States*
676 *Government. Neither the United States Government nor any agency thereof, nor any of their employees, makes any warranty,*
677 *express or implied, or assumes any legal liability or responsibility for the accuracy, completeness, or usefulness of any*
678 *information, apparatus, product, or process disclosed, or represents that its use would not infringe privately owned rights.*
679 *Reference herein to any specific commercial product, process, or service by trade name, trademark, manufacturer, or*
680 *otherwise does not necessarily constitute or imply its endorsement, recommendation, or favoring by the United States*
681 *Government or any agency thereof. The views and opinions of authors expressed herein do not necessarily state or reflect*
682 *those of the United States Government or any agency thereof."*

683 **References**

684 Abis, L., Loubet, B., Ciuraru, R., Lafouge, F., Houot, S., Nowak, V., Tripied, J., Dequiedt, S., Maron, P. A. and Sadet-
685 Bourgeteau, S.: Reduced microbial diversity induces larger volatile organic compound emissions from soils, Sci. Rep., 10(1),
686 6104, 2020.

687 Birch, H. F.: The effect of soil drying on humus decomposition and nitrogen availability, Plant Soil, 10(1), 9–31, 1958.

688 Burton, D. L. and Beauchamp, E. G.: Profile nitrous oxide and carbon dioxide concentrations in a soil subject to freezing,
689 Soil Sci. Soc. Am. J., 58, 115–122, 1994.

690 Bzowski, J., Kestin, J., Mason, E. A. and Uribe, F. J.: Equilibrium and transport properties of gas mixtures at low density:
691 eleven polyatomic gases and five noble gases, J. Phys. Chem. Ref. Data, 19(5), 1179–1232, 1990.

692 Citron, C. A., Gleitzmann, J., Laurenzano, G., Pukall, R. and Dickschat, J. S.: Terpenoids are widespread in actinomycetes: a
693 correlation of secondary metabolism and genome data, Chembiochem, 13(2), 202–214, 2012.

694 Conrad, R.: Quantification of methanogenic pathways using stable carbon isotopic signatures: a review and a proposal, Org.
695 Geochem., 36(5), 739–752, 2005.

https://doi.org/10.5194/bg-2020-401
Preprint. Discussion started: 28 December 2020

696 DeSutter, T. M., Sauer, T. J. and Parkin, T. B.: Porous tubing for use in monitoring soil CO_2 concentrations, Soil Biol.
697 Biochem., 38(9), 2676–2681, 2006.

698 Dhanumalayan, E. and Joshi, G. M.: Performance properties and applications of polytetrafluoroethylene (PTFE)—a review,
699 Adv. Compos. Hybr. Mater., 1(2), 247–268, 2018.

700 Flechard, C. R., Neftel, A., Jocher, M., Ammann, C., Leifeld, J. and Fuhrer, J.: Temporal changes in soil pore space CO_2
701 concentration and storage under permanent grassland, Agric. For. Meteorol., 142(1), 66–84, 2007.

702 Gangi, L., Rothfuss, Y., Ogée, J., Wingate, L., Vereecken, H. and Brüggemann, N.: A new method for in situ measurements
703 of oxygen isotopologues of soil water and carbon dioxide with high time resolution, Vadose Zone J., 14(8), vzj2014.11.0169,
704 2015.

705 Gonzalez-Meler, M. A., Rucks, J. S. and Aubanell, G.: Mechanistic insights on the responses of plant and ecosystem gas
706 exchange to global environmental change: lessons from Biosphere 2, Plant Sci., 226, 14–21, 2014.

707 Groffman, P. M., Butterbach-Bahl, K., Fulweiler, R. W., Gold, A. J., Morse, J. L., Stander, E. K., Tague, C., Tonitto, C. and
708 Vidon, P.: Challenges to incorporating spatially and temporally explicit phenomena (hotspots and hot moments) in
709 denitrification models, Biogeochemistry, 93(1), 49–77, 2009.

710 Guenther, A., Hewitt, C. N., Erickson, D., Fall, R., Geron, C., Graedel, T., Harley, P., Klinger, L., Lerdau, M., Mckay, W.
711 A., Pierce, T., Scholes, B., Steinbrecher, R., Tallamraju, R., Taylor, J. and Zimmerman, P.: A global model of natural
712 volatile organic compound emissions, J. Geophys. Res., 100(D5), 8873, 1995.

713 Gut, A., Blatter, A., Fahrni, M., Lehmann, B. E., Neftel, A. and Staffelbach, T.: A new membrane tube technique (METT)
714 for continuous gas measurements in soils, Plant Soil, 198(1), 79–88, 1998.

715 Hirsch, A. I., : Trumbore, S. E. and Goulden, M. L.: The surface CO_2 gradient and pore-space storage flux in a high-porosity
716 litter layer, Tellus B Chem Phys Meteorol, 56(4), 312–321, doi:10.3402/tellusb.v56i4.16449, 2004.

717 Holter, P.: Sampling air from dung pats by silicone rubber diffusion chambers, Soil Biol. Biochem., 22(7), 995–997, 1990.

718 Insam, H. and Seewald, M. S. A.: Volatile organic compounds (VOCs) in soils, Biol. Fertil. Soils, 46(3), 199–213, 2010.

719 Jacinthe, P.-A. and Dick, W. A.: Use of silicone tubing to sample nitrous oxide in the soil atmosphere, Soil Biol. Biochem.,
720 28(6), 721–726, 1996.

721 Jiao, S., Chen, W., Wang, J., Du, N., Li, Q. and Wei, G.: Soil microbiomes with distinct assemblies through vertical soil
722 profiles drive the cycling of multiple nutrients in reforested ecosystems, Microbiome, 6(1), 146, 2018.

723 Jochheim, H., Wirth, S. and von Unold, G.: A multi-layer, closed-loop system for continuous measurement of soil CO_2
724 concentration, J. Plant Nutr. Soil Sci., 181(1), 61–68, 2018.

725 Kammann, C., Grünhage, L. and Jäger, H.-J.: A new sampling technique to monitor concentrations of CH_4, N_2O and CO_2 in
726 air at well-defined depths in soils with varied water potential, Eur. J. Soil Sci., 52(2), 297–303, doi:10.1046/j.1365-
727 2389.2001.00380.x, 2001.

728 Karbin, S., Guillet, C., Kammann, C. I. and Niklaus, P. A.: Effects of long-term CO_2 enrichment on soil-atmosphere CH_4
729 fluxes and the spatial micro-distribution of methanotrophic bacteria, PLoS One, 10(7), e0131665, 2015.

730 Krämer, H. and Conrad, R.: Measurement of dissolved H_2 concentrations in methanogenic environments with a gas
731 diffusion probe, FEMS Microbiol. Ecol., 12(3), 149–158, 1993.

732 Krechmer, J., Lopez-Hilfiker, F., Koss, A., Hutterli, M., Stoermer, C., Deming, B., Kimmel, J., Warneke, C., Holzinger, R.,
733 Jayne, J., Worsnop, D., Fuhrer, K., Gonin, M. and de Gouw, J.: Evaluation of a new reagent-ion source and focusing ion–
734 molecule reactor for use in Proton-Transfer-Reaction Mass Spectrometry, Anal. Chem., 90(20), 12011–12018, 2018.

735 Leitner, S., Homyak, P. M., Blankinship, J. C., Eberwein, J., Jenerette, G. D., Zechmeister-Boltenstern, S. and Schimel, J. P.:
736 Linking NO and N_2O emission pulses with the mobilization of mineral and organic N upon rewetting dry soils, Soil Biol.
737 Biochem., 115, 461–466, 2017.

738 Maier, M., Schack-Kirchner, H., Aubinet, M., Goffin, S., Longdoz, B. and Parent, F.: Turbulence effect on gas transport in
739 three contrasting forest soils, Soil Sci. Soc. Am. J., 76(5), 1518–1528, 2012.

740 Massman, W. J.: A review of the molecular diffusivities of H_2O, CO_2, CH_4, CO, O_3, SO_2, NH_3, N_2O, NO, and NO_2 in air, O2
741 and N_2 near STP, Atmos. Environ., 32(6), 1111–1127, doi:10.1016/s1352-2310(97)00391-9, 1998.

742 **MATLAB,** 2018. 9.7.0.1190202 (R2019b), Natick, Massachusetts: The MathWorks Inc.

743 McCalley, C. K., Woodcroft, B. J., Hodgkins, S. B., Wehr, R. A., Kim, E.-H., Mondav, R., Crill, P. M., Chanton, J. P., Rich,
744 V. I., Tyson, G. W. and Saleska, S. R.: Methane dynamics regulated by microbial community response to permafrost thaw,
745 Nature, 514(7523), 478–481, 2014.

McClellan, M. J.: Estimating regional nitrous oxide emissions using isotopic ratio observations and a Bayesian inverse framework, Ph.D, Massachusetts Institute of Technology. [online] Available from: https://dspace.mit.edu/handle/1721.1/119986 (Accessed 8 September 2020), 2018.

McManus, J. B., Nelson, D. D. and Zahniser, M. S.: Design and performance of a dual-laser instrument for multiple isotopologues of carbon dioxide and water, Opt. Express, 23(5), 6569–6586, 2015.

McSharry, C., Faulkner, R., Rivers, S., Shaffer, M. S. P. and Welton, T.: The chemistry of East Asian lacquer: A review of the scientific literature, Stud Conserv, 52(sup1), 29–40, 2007.

Mohn, J., Wolf, B., Toyoda, S., Lin, C.-T., Liang, M.-C., Brüggemann, N., Wissel, H., Steiker, A. E., Dyckmans, J., Szwec, L., Ostrom, N. E., Casciotti, K. L., Forbes, M., Giesemann, A., Well, R., Doucett, R. R., Yarnes, C. T., Ridley, A. R., Kaiser, J. and Yoshida, N.: Interlaboratory assessment of nitrous oxide isotopomer analysis by isotope ratio mass spectrometry and laser spectroscopy: current status and perspectives, Rapid Commun. Mass Spectrom., 28(18), 1995–2007, 2014.

Munksgaard, N. C., Wurster, C. M. and Bird, M. I.: Continuous analysis of δ^{18} O and δD values of water by diffusion sampling cavity ring-down spectrometry: a novel sampling device for unattended field monitoring of precipitation, ground and surface waters, Rapid Commun. Mass Spectrom., 25(24), 3706–3712, doi:10.1002/rcm.5282, 2011.

Panikov, N. S., Mastepanov, M. A. and Christensen, T. R.: Membrane probe array: Technique development and observation of CO_2 and CH_4 diurnal oscillations in peat profile, Soil Biol. Biochem., 39(7), 1712–1723, 2007.

Parent, F., Plain, C., Epron, D., Maier, M. and Longdoz, B.: A new method for continuously measuring the δ^{13}C of soil CO_2 concentrations at different depths by laser spectrometry, Eur. J. Soil Sci., 64(4), 516–525, doi:10.1111/ejss.12047, 2013.

Penger, J., Conrad, R. and Blaser, M.: Stable carbon isotope fractionation by methylotrophic methanogenic archaea, Appl. Environ. Microbiol., 78(21), 7596–7602, 2012.

Peñuelas, J., Asensio, D., Tholl, D., Wenke, K., Rosenkranz, M., Piechulla, B. and Schnitzler, J. P.: Biogenic volatile emissions from the soil, Plant Cell Environ., 37(8), 1866–1891, 2014.

Petersen, S. O.: Diffusion probe for gas sampling in undisturbed soil, Eur. J. Soil Sci., 65(5), 663–671, 2014.

Raza, W., Mei, X., Wei, Z., Ling, N., Yuan, J., Wang, J., Huang, Q. and Shen, Q.: Profiling of soil volatile organic compounds after long-term application of inorganic, organic and organic-inorganic mixed fertilizers and their effect on plant growth, Sci. Total Environ., 607-608, 326–338, 2017.

772 Rock, L., Ellert, B. H., Mayer, B. and Norman, A. L.: Isotopic composition of tropospheric and soil N_2O from successive
773 depths of agricultural plots with contrasting crops and nitrogen amendments, J. Geophys. Res. D: Atmos., 112(D18),
774 doi:10.1029/2006JD008330, 2007.

775 Roscioli, J. R., Yacovitch, T. I., Floerchinger, C., Mitchell, A. L., Tkacik, D. S., Subramanian, R., Martinez, D. M., Vaughn,
776 T. L., Williams, L., Zimmerle, D. and Others: Measurements of methane emissions from natural gas gathering facilities and
777 processing plants: measurement methods, Atmos. Meas. Tech., 8(5), doi:10.5194/amt-8-2017-2015, 2015.

778 Rothfuss, F. and Conrad, R.: Development of a gas diffusion probe for the determination of methane concentrations and
779 diffusion characteristics in flooded paddy soil, FEMS Microbiol. Ecol., 14(4), 307–318, 1994.

780 Rothfuss, Y., Vereecken, H. and Brüggemann, N.: Monitoring water stable isotopic composition in soils using gas-
781 permeable tubing and infrared laser absorption spectroscopy, Water Resour. Res., 49(6), 3747–3755,
782 doi:10.1002/wrcr.20311, 2013.

783 Rothman, L. S., Gordon, I. E., Babikov, Y., Barbe, A., Benner, D. C., Bernath, P. F., Birk, M., Bizzocchi, L., Boudon, V.,
784 Brown, L. R. and Others: The HITRAN2012 molecular spectroscopic database, J. Quant. Spectrosc. Radiat. Transf., 130, 4–
785 50, 2013.

786 Saleska, S. R., Shorter, J. H., Herndon, S., Jiménez, R., Barry McManus, J., William Munger, J., Nelson, D. D. and Zahniser,
787 M. S.: What are the instrumentation requirements for measuring the isotopic composition of net ecosystem exchange of CO_2
788 using eddy covariance methods?, Isot. Environ. Health Stud., 42(2), 115–133, doi:10.1080/10256010600672959, 2006.

789 Schimel, J. P.: Life in dry soils: Effects of drought on soil microbial communities and processes, Annu. Rev. Ecol. Evol.
790 Syst., doi:10.1146/annurev-ecolsys-110617-062614, 2018.

791 Schulz-Bohm, K., Zweers, H., de Boer, W. and Garbeva, P.: A fragrant neighborhood: volatile mediated bacterial
792 interactions in soil, Front. Microbiol., 6, 1212, 2015.

793 Schulz-Bohm, K., Gerards, S., Hundscheid, M., Melenhorst, J., de Boer, W. and Garbeva, P.: Calling from distance:
794 attraction of soil bacteria by plant root volatiles, ISME J., 12(5), 1252–1262, 2018.

795 Snider, D. M., Venkiteswaran, J. J., Schiff, S. L. and Spoelstra, J.: From the ground up: Global nitrous oxide sources are
796 constrained by stable isotope values, PLOS ONE, 10(3), e0118954, doi:10.1371/journal.pone.0118954, 2015.

https://doi.org/10.5194/bg-2020-401
Preprint. Discussion started: 28 December 2020

797 Sutka, R. L., Ostrom, N. E., Ostrom, P. H., Breznak, J. A., Gandhi, H., Pitt, A. J. and Li, F.: Distinguishing nitrous oxide
798 production from nitrification and denitrification on the basis of isotopomer abundances, Appl. Environ. Microbiol., 72(1),
799 638–644, 2006.

800 Team, R. C.: R Core Team (2017). R: A language and environment for statistical computing, R Found. Stat. Comput.
801 Vienna, Austria, 2017.

802 Toyoda, S., Yoshida, N. and Koba, K.: Isotopocule analysis of biologically produced nitrous oxide in various environments,
803 Mass Spectrom. Rev., 36(2), 135–160, 2017.

804 Van Haren, J. L. M., Handley, L. L., Biel, K. Y., Kudeyarov, V. N., McLain, J. E. T., Martens, D. A. and Colodner, D. C.:
805 Drought-induced nitrous oxide flux dynamics in an enclosed tropical forest, Glob. Chang. Biol., 11(8), 1247–1257, 2005.

806 Voglar, G. E., Zavadlav, S., Levanič, T. and Ferlan, M.: Measuring techniques for concentration and stable isotopologues of
807 CO2 in a terrestrial ecosystem: A review, Earth-Sci. Rev., 199, 102978, 2019.

808 Volkmann, T. H. M. and Weiler, M.: Continual in situ monitoring of pore water stable isotopes in the subsurface, Hydrol.
809 Earth Syst. Sci., 18(5), 1819–1833, 2014.

810 Volkmann, T. H. M., Kühnhammer, K., Herbstritt, B., Gessler, A. and Weiler, M.: A method for in situ monitoring of the
811 isotope composition of tree xylem water using laser spectroscopy, Plant, Cell & Environ., 39(9), 2055–2063,
812 doi:10.1111/pce.12725, 2016a.

813 Volkmann, T. H. M., Haberer, K., Gessler, A. and Weiler, M.: High-resolution isotope measurements resolve rapid
814 ecohydrological dynamics at the soil plant interface, New Phytol., 210(3), 839–849, 2016b.

815 Volkmann, T. H. M., Sengupta, A., Pangle, L. A., Dontsova, K., Barron-Gafford, G. A., Harman, C. J., Niu, G.-Y.,
816 Meredith, L. K., Abramson, N., Neto, A. A. M. and Others: Controlled experiments of hillslope coevolution at the Biosphere
817 2 Landscape Evolution Observatory: Toward prediction of coupled hydrological, biogeochemical, and ecological change, in
818 Hydrology of Artificial and Controlled Experiments, edited by W.-Z. G. Jiu-Fu Liu, pp. 25–74, IntechOpen., 2018.

819 Wang, Y., Hu, C., Ming, H., Oenema, O., Schaefer, D. A., Dong, W., Zhang, Y. and Li, X.: Methane, carbon dioxide and
820 nitrous oxide fluxes in soil profile under a winter wheat-summer maize rotation in the north china plain, PLoS ONE, 9(6),
821 e98445, doi:10.1371/journal.pone.0098445, 2014.

https://doi.org/10.5194/bg-2020-401
Preprint. Discussion started: 28 December 2020

822 Wei, J., Ibraim, E., Brüggemann, N., Vereecken, H. and Mohn, J.: First real-time isotopic characterisation of N_2O from
823 chemodenitrification, Geochim. Cosmochim. Acta, 267, 17–32, 2019.

824 Werle, P., Mucke, R. and Slemr, F.: The limits of signal averaging in atmospheric trace-gas monitoring by tunable diode-
825 laser absorption spectroscopy (TDLAS), Applied Physics B, 57(2), 131–139, doi:10.1007/bf00425997, 1993.

826 Wester-Larsen, L., Kramshøj, M., Albers, C. N. and Rinnan, R.: Biogenic volatile organic compounds in arctic soil: A field
827 study of concentrations and variability with vegetation cover, J. Geophys. Res. Biogeosci., 125(7), 36, 2020.

828 Yoshida, N. and Toyoda, S.: Constraining the atmospheric N_2O budget from intramolecular site preference in N_2O
829 isotopomers, Nature, 405(6784), 330–334, 2000.